3. Blast vibrations

Session 4

Brighton Conference Proceedings 2005, R. Holmberg et al

Influence of burden size on blast-induced ground vibrations in open-cast mines

M. Ramulu, A.K. Chakraborty, A.K. Raina, P.B. Choudhury & C. Bandopadhyay
Central Mining Research Institute Regional Centre, Nagpur, India

N.R. Thote
Department of Mining Engineering, Visvesvaraya National Institute of Technology, Nagpur, India

ABSTRACT: Ground vibrations have haunted blasting engineers ever since environmental concerns attained significant importance. Based on the plethora of research activity on the subject, different criteria have been designed to specify limits of blast-induced ground vibrations. In spite of the significant research, the criteria vary from one place to another and are not foolproof. This is primarily because of varied rock and blasting conditions. To augment the existing knowledge base, investigations have been carried out in three open-cast mines of Western Coalfields Limited (WCL), Singareni Collieries Company Limited (SCCL) and L&T (the Naokari limestone quarry) to establish the effect of the burden on ground vibrations and air overpressure. The study revealed that the burden has an appreciable influence on the blast-induced vibrations. Vibration data were subjected to statistical analysis for correlation of the peak particle velocity and excess burden. The excess burden has a key influence on peak particle velocity. A vibration database specially generated for almost equal-scale distance was correlated with the peak particle velocity and the burden. The study provides an interesting insight into the influence of excess burden on the peak particle velocity of vibrations.

1 INTRODUCTION

The present predictor equation does not address the effect of various blast design parameters on ground vibrations. Although the effect of blast design parameters has been broadly considered by many researchers (Siskind *et al.* 1980, du Pont 1977) in deriving the vibration predictor equation, in terms of negative power of scaled distance, relevant weight has not been assigned to other blast design parameters such as the burden, spacing and bench height. It is a recognised fact that the burden makes its own contribution to blast vibrations (Ramulu 1998, Raina *et al.* 1999). Researchers from USBM also suggested that more studies are required firmly to establish the effect of blast design parameters, especially the burden, on the intensity of the peak particle velocity, V_{max}, of vibrations (Crum 1997). Controlling blast vibrations through blast design modification, in particular the blast geometry which includes burden and spacing, has been a topic of interest to researchers such as Anderson *et al.* (1985) and Wiss (1978).

According to Jimeno (1995), if the confinement or burden is excessive, the energy from the explosion has too much resistance for effective fracture and displacement of the rock. Part of the energy becomes seismic and intensifies the vibrations more than if there were a free face for rock displacement.

Avoiding too much burden has become one of the measures for reducing ground vibrations (Scott

1996, Persson 1994, p. 350). Sames (1999) revealed that design parameters such as delay time, burden, initiation sequence and decoupling charges considerably alter the dispersion of seismic energy. The effect of burden on vibrations has been indicated in a number of research works worldwide (Siskind *et al.* 1980, Gordon *et al.* 1997, Crum 1997). It is interesting to note that the effect of blast design parameters on vibrations was predominant in nearfield observations, while at far distances the geological features control the amplitude of vibrations (Nutting 1997). CMRI, in a number of field studies, discovered that ground vibrations and air overpressure are very sensitive to blast design parameters, especially the burden which contributes to confinement (CMRI Report 1998). Sometimes there exists excess burden owing to faulty drilling and the collapse of one or more drill holes before charging.

According to Floyd (1997), the major cause of elevated ground vibrations is the overconfinement of explosive energy when the blasthole detonates. This overconfinement causes a large portion of the energy to be absorbed by the rock mass instead being utilised for fragmentation and muckpile displacement. The excess energy absorbed by the rock mass results in enhancement of ground vibrations. Along with lack of free faces and insufficient delay interval between rows, excessively large blasthole burden dimensions and toe burdens are the major causes of overconfinement. Excessively large burdens obviously result in low powder factors.

Anderson (1985) found, at the same recording location, a totally confined single-charge shot will produce about twice the peak particle velocity of a nearby free-face single-charge shot.

Dick (1983) revealed that, in addition to the charge weight per delay, the distance and the delay interval, two factors may affect the level of ground vibrations at a given location. The first is overconfinement. A charge with a properly designed burden will produce less vibration per pound of explosive than a charge with too much burden. An excessive amount of subdrilling, which results in an extremely heavy confinement of the explosive charge, will also cause higher levels of ground vibration, particularly if the primer is placed in the subdrilling. In multiple-row blasts, there is a tendency for the later rows to become overconfined. To avoid this, it is often advisable to use longer delay periods between these later rows to give better relief. Therefore, to reduce the intensity of the vibrations, overly confined charges such as those having too much burden or too much subdrilling should be avoided.

In keeping with the above assertions, the present investigation was initiated at the Kamptee open-cast mine (KOC mine), WCL, the Prakasham Khani open-cast mine (PKOC mine), SCCL, and the Naokari limestone quarry (NL quarry), L&T, India. The details of the site, field investigations and data generation and analysis are explained in the following chapters.

2 DETAILS OF THE EXPERIMENTATION SITES

2.1 KOC mine

There are two overburden (OB) benches and two coal benches in Kamptee open-cast mine (KOC mine). The method of mining is by shovel–dumper combination. The gradient of the coal seam is 1 in 4, and the advance of the mine is in the direction of strike. The deeper portion below a depth of 100 m has been worked out by underground mining. The average blasthole depth is 8.5 m and the diameter is 150 mm. The blasting was done by slurry explosives. The KOC mine has a lithology of clay, sandstone and coal from top to bottom, as seen in the exposed sections. The clay/soil is compact and sandy in nature and has a restricted thickness of 2–3 m. Sandstone is predominant, with variations from coarse to pebbly to fine grained. The colour of the sandstone varies from grey to yellowish to reddish brown. Hard and compact ferruginous sandstone layers are seen frequently in the section. Shale is also observed in the section between sandstone layers. The formation is mostly dry, with dripping or wet conditions in a few places.

2.2 PKOC mine, SCCL

The PKOC mine is located at Manuguru which is at a distance of about 60 km north-east of Kothagudem and about 50 km north-west of Bhadrachalam, a famous temple town. The approximate longitude and latitude of the mine are 80˚50′ and 17˚55′ respectively. It is one of the biggest open-cast mines of the SCCL, with an annual production of 2.75 Mt of coal and 7.5 Mm^3 of OB. The type and quality of coal are bituminous and C-grade (mostly) respectively.

2.2.1 *Method of working*

The mine is divided into two sections called East and West. The investigation was carried out in the East section, owing to the availability of more benches for trial blasts. There are five working benches of OB (benches 1–5 with bench 1 as the top bench), in addition to a coal bench in the East section. The method of mining is by drilling and blasting, and OB removal is by shovel–dumper combination. The specific charge of explosive used for blasting is 0.41–0.47 kg/m^3 in all the OB benches. Site mixed slurry explosive was used for trial blasts in all the benches except for bench 2, where cartridged slurry explosive was used owing to the watery conditions.

2.2.2 *Geology and rock mass properties*

The general geological features of the OB were studied by visual inspection. Schmidt hammer testing was carried out to estimate *in situ* strength. The primary lithology of the mine is sandstone of varying strength and with varying joint spacing and joint condition. Benches 1 and 2 are composed of coarse-grained, blocky, pinkish sandstone. Benches 3 and 4 are, however, of composite nature, with blocky to bedded sandstones and crushed shales with slickensided and highly undulating beds representing local folding and faulting. The uniaxial compressive strength (UCS) of the sandstone varies from 20 to 40 MPa, whereas that of the shale ranges from 20 to 30 MPa. Some greenish, highly imbricated and lumpy volcano-sedimentary material is present at places in bench 4, which is indicative of geological hiatus, and slickensided faulting is inevitable.

2.3 *NL quarry*

The NL quarry is a semi-mechanised mine, which is the source of feed to the Awarpur Cement Works, L&T (Larsen & Toubro Ltd). The location of the quarry is at about 25 km south of Chandrapur town in Maharashtra. The mine is presently operated on the North and South side of the leasehold. The mine is operating with six benches, numbered 1–6 in descending order. Geologically, the mine comprises different limestone grades from top to bottom, with greater fracture intensity in the lower benches (benches 3–6). The top or first bench is weathered and has *in situ* boulders owing to clastic formation. Occasional voids are also found in this bench owing to the above effect. The limestone has thus hardened and, because of departure from the normal limestone structure, the bench is comparatively difficult to blast. The limestone is folded in an anticline fashion, with local folding in the limbs. Three prominent joint sets can be observed, thereby creating definite blocks of tabular shapes with dimensional variation from one place to another in the first and second benches. The other benches (3–6) show quite uniform block sizes of tabular shape and are relatively easy to blast. The blast design parameters prevailing at the mine are given in Table 1.

3 TRIAL BLASTS AND DATA GENERATION

3.1 *KOC mine*

A total of 30 trial blasts were conducted, with the burden varying from 4 to 9 m. The optimum burden was considered to be 5 m for the particular strata. The vibration was monitored by two seismographs placed at two different distances in the same direction from the blast. The maximum charge per delay and round was kept constant for all six blasts. The design details of the trial blasts are mentioned in Table 1.

3.2 *PKOC mine*

Twelve trial blasts were conducted and the V_{max} and P were monitored with two seismographs. The data recorded include most of the characteristics of vibration and P, such as peak V_{max}, acceleration, frequency and wavelength. The optimum burden was calculated to be 5.8 m by the optimization techniques already explained. The actual burden varied from 5.5 to 13 m. The scaled distance varied from 0.44 to 0.46. The designed scaled distance was 0.45, and the actual scaled distance deviated by 0.1 owing to some unavoidable practical difficulties. The design details of the trial blasts are mentioned in Table 1.

3.3 *NL quarry*

The vibration data were generated with varying burdens of three benches of the limestone quarry. Three seismographs were fixed at three different distances from the blast site. All the monitoring stations were fixed at the rear side of the blast site strategically to maintain constant scaled distance in each direction. This is done to avoid the effect of distance and charge per delay on the vibrations. In order to establish the effect of burden on the

intensity of ground vibration, the effect of other input parameters should be nullified. The effects of geological features and the properties of the medium were almost eliminated by selecting the monitoring stations in the same direction. The effect of the medium could not be eliminated completely because of the slight change in location of the blast site, which led to a corresponding change in the path of the vibrations. Vibration monitoring was carried out at three different distances: 170, 270 and 550 m. The scaled distance at 170 m ranged from 14.8 to 15.7 m/kg$^{0.5}$, with a standard deviation of 0.4. The scaled distance at 270 m ranged from 24.1 to 25.0 m/kg$^{0.5}$, with a standard deviation of 0.4. The scaled distance at 550 m ranged from 49.2 to 50 m/kg$^{0.5}$, with a standard deviation of 0.5. On the basis of rock mass characterisation, the optimum burden calculated for the limestone quarry was 4 m. A burden that exceeded 4 m was considered to be excess burden. The excess burden varied from 4 to 8.3 m in all the experiments. The total number of blasts monitored was 15, and the total number of vibration events monitored was 45. Of these, a few readings were omitted from the analysis because of their abnormal values. This may have been due to instrument fixation errors and errors related to false triggering of the instrument. The charge per delay, as well as the charge per round, was maintained constant for all 15 blasts. The number of rows in each round was 2.

4 DATA ANALYSIS AND RESULTS

The field data collected from the mine, was subjected to analysis in order to establish the influence of the burden on V_{max} and its frequency, f_v. The details of the analysis and results are given below.

The complete data generated with both optimum burden and excess burden were analysed in order to find the trend line of Vmax versus scaled distance (SD). The Vmax–SD curve is shown in Figure 1. To determine the influence of burden at a preliminary level, trend lines were drawn for Vmax versus SD with both optimum burden and excess burden and are shown in Figure 2. All the data collected during the experimentation were included in the analysis. The following inferences can be drawn from the regression analysis of V_{max} and SD data.

The regression analysis of the combined V_{max} and SD data with both optimum burden and overburden gives a poor correlation (R^2=0.28) owing to scattering of the V_{max} levels. The scattering of V_{max} data may be due to the influence of excess burden for some of the trial blasts. Except for a few points, there are two separate clusters of points with optimum burden and overburden, which indicates the influence of overburden on the V_{max} levels. All the V_{max} data with excess burden are clearly above the V_{max} data with optimum burden. The correlation was improved considerably after separating V_{max} data with respect to burden.

The relatively poor correlation (R^2 = 0.51) for the data with excess burden indicates that scattering of the V_{max} levels may be due to the differing influence of excess burden at various distances.

The vibration data were also analysed in order to establish the influence of burden at different distances.

The plot of V_{max} versus burden is shown in Figure 3 for both 200 and 300 m. Out of 10 field observations, no observation was rejected for both 200 and 300 m analysis. The R^2 of V_{max} and burden data is 0.92 for 200 m and 0.44 for 300 m distance. The gradient of the curve for 200 m is steeper than that of the curve for 300 m.

The relatively very good correlation (R^2 = 0.92) for V_{max} levels at 200 m distance indicates that the degree of influence of excess burden is consistent at lower distances. The plots of f_v versus burden for both 200 and 300 m are shown in Figure 4. All 10 field observations were considered for analysis. The R^2 of f_v and burden data is 0.13 for 200 m and 0.03 for 300 m.

The following inferences can be drawn from the regression analysis of V_{max} and f_v versus burden:

- The relatively higher power (steep gradient) for V_{max} levels at 200 m distance indicates that the degree of influence of excess burden is greater at shorter distances.

- Some observations with suboptimum burdens indicate that there is a decrease in vibration levels with a decrease in burden.

- There is no influence of burden on the frequency of vibration as the R^2 of f_v versus burden is negligible for both the distances.

4.2 PKOC mine

The plot of V_{max} versus burden is shown in Figure 5. Out of 12 field observations, no data were rejected for V_{max} analysis except for one V_{max} observation which was generated without free face (crater blast). The vibration recorded for crater blast at the same scaled distance was 40.1 mm/s. The correlation coefficient, R^2, of V_{max} and burden data is 0.97, which is treated as an excellent relationship.

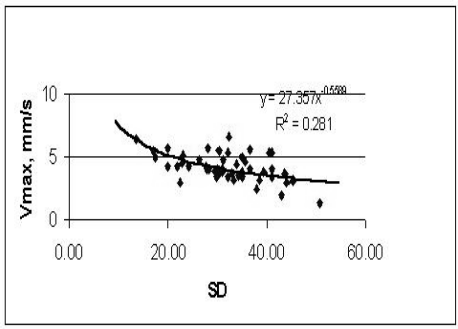

Figure 1 V_{max} versus square root scaled distance for combined data of optimum burden and excess burden

Figure 1. Vmax versus root scaled distance for combined data of optimum burden and excess burden.

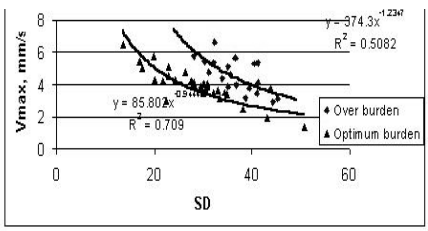

Figure 2 Vmax versus square root scaled distance with optimum burden and excess burden

Figure 2. Vmax versus square root scaled distance with optimum burden and excess burden.

- Relatively very good correlation (R^2=0.97) for V_{max} versus burden indicates that there is very good influence of burden on vibration.
- The vibration is directly proportional to the burden. The crater blast vibration of 40.1 mm/s indicate that the increase in vibration after certain point of excess burden may be insignificant.

The plots of f_v versus burden are shown in Figure 6. All the field observations recorded were considered for the analysis. The R^2 of f_v versus burden is 0.2.

The following inference can be drawn from the regression analysis of f_v versus burden: the poor correlation (R^2 = 0.2) between f_v and burden data indicates that there is no influence of burden on f_v.

4.3 NL quarry

The vibration data at the NL quarry were subjected to regression analysis in order to establish the influence of burden at three different distances.

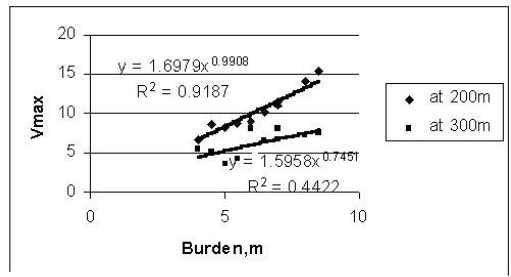

Figure 3. Vmax versus burden at 200m and 300m at KOC mine.

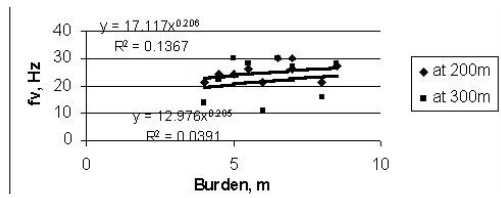

Figure 4. fv versus burden at 200m and 300m at KOC mine.

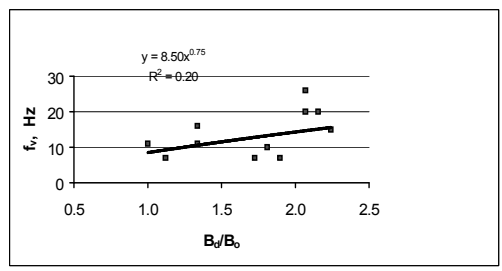

Figure 5. V_{max} versus burden ratio at the SCCL mine.

The plot of V_{max} versus burden at 170, 270 and 550 m is shown in Figure 7. The R^2 values are 0.86, 0.72 and 0.50 for 170, 270 and 550 m distances respectively. The plot of f_v versus burden is shown in Figure 8. The R^2 of f_v and burden is

0.1, 0.46 and 0.27 at 170, 270 and 550 m respectively.

The following inferences can be drawn from the regression analysis of V_{max} and f_v versus burden:

- The trend lines show that there is significant influence of burden on V_{max}.
- The relatively better correlation for shorter distances indicates that the degree of influence of burden is consistent at smaller distances.
- The relatively higher power (steep gradient) for V_{max} levels at lower distances indicates that the degree of influence of burden is greater at smaller distances.
- There is negligible influence of burden on the frequency of vibration as the R^2 is poor for all the distances.

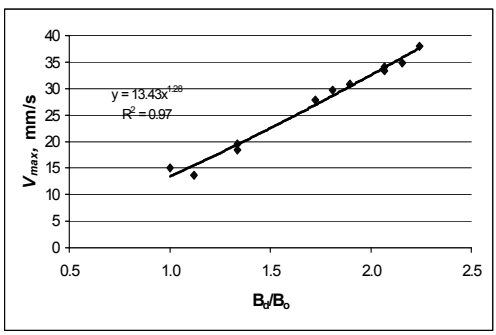

Figure 6. Frequency of vibration, f_v, versus burden at the SCCL mine.

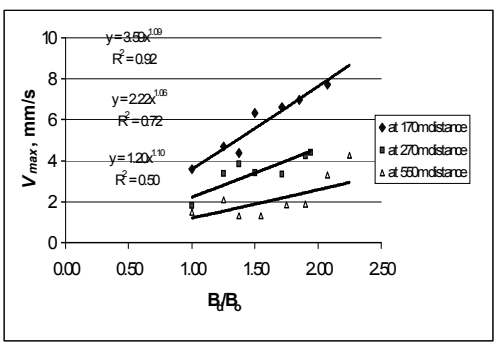

Figure 7. Vibration versus burden ratios for the NL quarry.

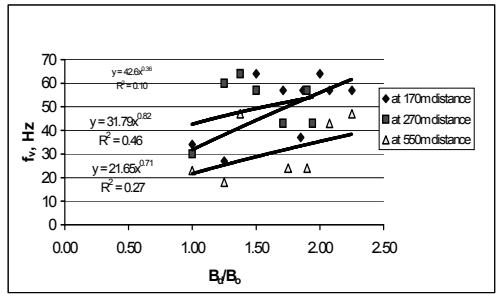

Figure 8. Frequency of vibration, f_v, versus burden for the NL quarry.

5 CONCLUSIONS

The following conclusions were drawn from the above experimental study at both coal mines. The conclusions can be categorized on the basis of the influence of burden on vibration and frequency.

- The study clearly indicates that the influence of burden on peak particle velocity of the ground vibrations is very significant.
- The burden is directly proportional to the peak particle velocity levels within the range of optimum burden to twice the optimum burden.
- Some observations with suboptimum burdens indicate that there is a decrease in vibration levels with a decrease of burden.
- The influence of burden on vibration is more significant at shorter distances than at greater distances.
- The influence of burden on vibration frequency is not insignificant.

5.1 ACKNOWLEDGEMENT

The authors express their sincere thanks to the Director, CMRI, for permission to publish this paper.

REFERENCES

Anderson, D.A., Ritter, A.P., Winzer, S.R. & Reil, J.W. 1985. A method for site specific prediction and control of ground vibration from blasting. In *Proc. 1st minisymposium on explosives and blasting research, San Diego, CA*: 28–43.

Crum, S.V., Siskind, D.E. & Eltschlager, K. 1997. Blast vibration measurements at far distances and design

influences on ground vibrations. In *Proc. annual conference on explosives and blasting research, explosives reference database on CD-ROM*, International Society of Explosive Engineers, Ohio.

Dick, R.A., Fletcher, L.R. & D'Andrea, D.V. 1983. *Explosives and Blasting Procedures Manual*, Bureau of Mines IC 8925.

du Pont, E.I. 1977. *Blasters Handbook*, 175th anniversary edition. Wilmington, Delaware: E.I. du Pont de Nemours, Inc.

Floyd, J.L. & Conn D.B. 1997. PhotoSeis – an advanced method for vibration analysis and control. In *Proc. annual conference on explosives and blasting research, explosives reference database on CD-ROM*, International Society of Explosive Engineers, Ohio.

Gordon, G. & Nies, D. 1997. Small borehole blasting in high liability locations. In *Proc. annual conference on explosives and blasting research, explosives reference database on CD-ROM*, International Society of Explosive Engineers, Ohio.

Jimeno, C.L., Jimeno, E.L. & Carcedo, F.J.A. 1995. *Drilling and Blasting of Rocks*: 183–184. Rotterdam, Balkema.

Nutting, M.J. & Froedge, D.T. 1997. The mapping of vibration patterns around a blast. In *Proc. annual conference on explosives and blasting research, explosives reference database on CD-ROM*, International Society of Explosive Engineers, Ohio.

Persson, P.A., Holmberg, R. & Lee, J. 1994. *Rock Blasting and Explosives Engineering*: CRC.

Raina, A.K., Ramulu, M., Chakraborty, A.K., Choudhury, P.B. & Jethwa, J.L. 1999. Monitoring and control of blast vibrations and fly rock at Kamptee OCP, WCL, Nagpur. CMRI internal report: 1–15.

Ramulu, M., Chakraborty, A.K., Raina, A.K., Choudhury, P.B., Jethwa, J.L. & Singh, T.N. 1998. CMRI report on blast induced ground vibration monitoring at Lakshmi cement limestone mines, Rajasthan: 1–10.

Sames 1999. The influnce of blast parameters on vibration and airblast. *Fragblast-99, Johansberg*, South African Institute of Mining and Metallurgy: 149–155.

Scott, A., Cokker, A., Djordjevic, N., Higgins, M., La Rosa, D., Sarma, K.S. & Wedmaier, R. 1996. Open pit blast design analysis and optimization. JKMRC monograph series in mining and mineral processing: 266–280.

Siskind, D.E., Stagg, M.S., Kopp, J.W. & Dowding, C.H. 1980. Structure response and damage produced by ground vibration from surface mine blasting. RI 8507, US Bureau of Mines.

Wiss, J.F. & Linehan, P.W. 1978. Control of vibrations and blast noise from surface coal mining. Volumes I–IV. Report to US Bureau of Mines, Bureau of Mines OFR 103-79.

Brighton Conference Proceedings 2005, R. Holmberg et al

The prediction of peak particle velocity vibration levels in underground structures that arise as a result of surface blasting

W.J. Birch, M. Pegden & T.J. White
Blasting and Environmental Research Group, Department of Mining, Quarrying and Minerals Engineering, The University of Leeds

J. Bradshaw
Whitwell Quarry, Lafarge Aggregates, Derbyshire

ABSTRACT: The Department of Mining, Quarrying and Mineral Engineering at the University of Leeds has a long history of research into the environmental impacts of blasting from quarries and open-cast mines. This paper seeks to build on the original detailed case study into the structural damaged induced in a rock-walled tunnel with a brick-lined crown owing to close-proximity quarry blasting. Currently, Network Rail (formerly Railtrack plc) in the United Kingdom usually imposes a vibration limit of 12 mm/s (peak particle velocity) on railway tunnels. This limit is based on research conducted by the United States Bureau of Mines (USBM) into the response of domestic buildings, which indicated that cosmetic or threshold damage has not been shown to occur below this level. The USBM research also indicates that structural damage may occur at levels of 50 mm/s and above. The original study, in combination with an evaluation of similar detailed published case studies, reappraised the vibration levels required to cause structural damage to railway tunnels and found that the value of 12 mm/s currently stipulated is extremely conservative However, it is extremely difficult to gain regular access to a live railway tunnel for the purposes of monitoring blasts. Therefore, what is required is a method of predicting the likely peak particle velocities at the tunnel from readings taken at an adjacent location. This study has been conducted at a quarry in Northern England with a railway tunnel in close proximity. A number of boreholes have been drilled in close proximity to the tunnel, with permanent triaxial geophones installed such that simultaneous readings could be taken at the surface and at various depths. The results clearly indicate that the peak particle velocities (PPVs) recorded at the surface are statistically different to those recorded at depth. However, while the intercept values of the respective log–log plot of PPV versus scaled distance are significantly different, the gradients are very similar. Thus, it becomes possible to predict the PPV values within the borehole from values observed at the surface and hence infer the likely values at an underground structure such as a tunnel.

1 INTRODUCTION

Blasting is a regular occurrence at many quarries and open-cast coal sites throughout the United Kingdom, where it is invariably considered by the operator to be an essential aspect of the economic extraction of minerals. In a densely populated country such as the United Kingdom, it is becoming impossible to use explosives without the environmental impacts affecting at least one structure. Quarrying companies face the problem of maximising reserves of rock or mineral without causing harm or nuisance to third-party structures (such as tunnels, ancient monuments, sensitive industrial installations and domestic properties). Accurate modelling and prediction of the effects of close-proximity blasting are therefore becoming increasingly important. Although much work has been carried out concerning the response of residential properties to blast-induced vibration in the United States by the former United States Bureau of Mines (USBM) (Nichollis et al.) and in the United Kingdom by Farnfield and White (1993), there has been very little investigation into

the response of railway tunnels and other similar structures.

Currently, Network Rail (formerly Railtrack plc in the United Kingdom) usually imposes a vibration limit of 12 mm/s (peak particle velocity) on railway tunnels. This limit is based on research conducted by the USBM into the response of domestic buildings, which indicated that cosmetic or threshold damage has not been shown to occur below this level. The USBM research also indicates that structural damage may occur at levels of 50 mm/s and above. The original study, in combination with an evaluation of similar detailed published case studies, reappraises the vibration levels required to cause structural damage to railway tunnels and indicates that the value of 12 mm/s currently stipulated is extremely conservative.

2 PREVIOUS WORK

In an attempt to determine the levels of vibration that can be safely imposed on tunnels and other similar structures, a detailed investigation was conducted by Kaslik *et al.* (2000) into the effects of close-proximity blasting on a disused railway tunnel in South Wales.

Taffs Well quarry is located in South Wales and has a disused railway tunnel (Walnut Tree) running through its south-east corner. Quarry development plans included the extension of the south-east corner and therefore the destruction of the central section of the tunnel. The aim of the original project was to investigate vibration levels at which damage occurred to the tunnel.

The project consisted of two phases:

- An investigation of existing blast damage to the tunnel, as a considerable amount of blasting had taken place adjacent to the tunnel prior to this study.
- A monitoring program consisting of detailed surveys, photographs and vibration recordings related to the response of the tunnel to each individual quarry blast.

Blast damage at the disused railway tunnel was examined and the blasts leading to the damage were analysed. In addition, the vibration effects on the tunnel of 33 blasts were monitored over a 1.5 year period. A total of 26 peak particle velocities above 50 mm/s from eight separate blasts were actually recorded on the tunnel lining, and it was estimated that 13 of the blasts would induce vibrations of more than 50 mm/s on the tunnel crown. Of the 33 blasts, only six caused visible damage to the tunnel (four of which were specifically designed to break into the tunnel).

Major damage to the tunnel occurred at an estimated vibration level of over 19,000 mm/s, and visible damage at over 14,000 mm/s. Permanent movement of the tunnel lining occurred at vibration levels of over 1000 mm/s, and the collapse of an already damaged area of brickwork occurred at over 600 mm/s. Recorded vibration levels of up to 306 mm/s and predicted levels of 390 mm/s were experienced on the tunnel crown without causing damage.

These results are consistent with the findings of Andrieux *et al.* (1996) who showed that overbreak occurs at PPVs of 3500–4500 mm/s, fresh fractures occur at PPVs of 850–1000 mm/s and PPVs of 300–400 mm/s can cause the extension of existing fractures.

The results are also consistent with estimates by Sakurai *et al.* (1977) which suggest that damage to a concrete tunnel lining would occur at a PPV of 350 mm/s, and by Dowding (1977) whose study into earthquake-induced damage to railway tunnels found no reports even of falling stones in unlined tunnels or cracking in lined tunnels up to 200 mm/s, and only a few incidences of minor cracking in concrete-lined tunnels at levels up to 370 mm/s. Clover (1986) reports on the findings of Labreche (1983) that vibrations of 460 mm/s were required to cause damage to unlined tunnels and Langerfors and Kihlstrom relate the fall of stones in galleries and tunnels to vibrations of 300 mm/s.

The two incidences of very minor damage recorded at vibration levels of 58 and 62 mm/s are consistent with findings of Tunstall (1997), who relates the damage observed to the RMR of the rock mass. His results show that for an RMR of 65–70, a PPV of 50–60 mm/s would be required to cause minor damage. They are also consistent with observations by Smith (1986), New (1989) and Olson (1972) who found that vibration levels of <50, <50 and 56 mm/s respectively caused no damage to tunnels.

It was concluded that a peak particle velocity limit of 50 mm/s would ensure that no damage occurs to a railway tunnel of similar design and condition within a similar rock mass.

3 CURRENT WORK

Having established by means of a detailed monitoring programme the vibration levels needed

to cause structural damage to the disused Walnut tunnel at Taff Well quarry, and finding that these equated well with existing case studies carried out by other researchers worldwide, the next section of the study needed to establish the relationship between PPV levels that can be monitored on the surface with those experienced below ground. The research project then moved to a new location. Whitwell quarry is situated south-east of Worksop on the border of Derbyshire and Nottinghamshire. The site, operated by Lafarge Aggregates, produces limestone aggregate for road stone, together with feed for its on-site rotary kilns. A railway tunnel is located in the northern section of the quarry area which effectively sterilises a significant quantity of the potential aggregate reserves of the quarry. As this is an operational railway line, it was not possible to gain direct access to the inside of the tunnel itself. Instead, six boreholes were drilled from the surface adjacent to the railway tunnel. Three triaxial arrays were permanently established in each borehole: the first at the surface, the second at crown level and the deepest at invert level. It is the modelling of these data and the subsequent interpretation that are central to this section of the work.

4 STATISTICAL ANALYSIS: APPLICATION OF THE LIKELIHOOD RATIO TEST

In order to diagnose any apparent difference and to quantify any such variation between surface and underground data subsets, a statistical method is required formally to carry out the analysis. A great deal of investigation into the application of various advanced statistical techniques has been carried by the Department of Mining, Quarrying and Mineral Engineering, University of Leeds, UK, and, through such work, dedicated analytical approaches have been promoted. For this particular investigation, a variant of the likelihood ratio test (Birch *et al.* 2004) was the application of choice. The following is a brief summary of the technique.

4.1 Maximum likelihood estimation

Maximum likelihood estimation (MLE) is the name given to the process for determining a parameter value that is most likely, given the data that have been observed. This is based upon a logical argument between 'probability' and likelihood' (Fisher 1925).

The procedure of least-squares estimation is broadly known and utilised. In particular, it is applied to scaled-distance regression curves and used to estimate the parameters for slope, intercept and variance. Another way to approach estimation is to specify how likely are the parameter value, given the data observed, and then to maximise the likelihood function. Where the least-squares method is used and the normal distribution is appropriate for scatter about the line, then the two methods are identical: maximising the likelihood is the same as minimising the sum of the squares of the residuals.

Such MLE values will rarely give exactly the same value, as some variability due to random data scatter will always be present, but, if indeed the subsequent blasts are carried out in the same manner as the first, then the degree of variability will be seen to be small and statistically insignificant. Alternatively, if the MLE values for two blasts are seen to be dramatically different, then this will indicate that some difference exists between the blasts. In other words, a difference exists in the assumed underlying conditional probability that the two blast models are the same.

4.2 Likelihood Ratio Test

Scaled-distance model fitting provides a framework from which we are able not only to estimate the maximum likelihood for parameters but also to test whether or not they are significantly different from other values. Suppose that data are available from two blast datasets. It is possible either to use a different pair of parameters (slope and intercept) for each dataset – a total of four parameters, or to use the same pair of parameters for both datasets – only two parameters. This is appropriate if the blast sites are similar. It is important to have a formal test to determine if four or two parameters are required. Here, the likelihood ratio test will be used.

The likelihood will be greater (and so the sum of squares of residuals will be smaller) if four parameters are fitted rather than just two. If the two blast models are not similar, then the increase in the likelihood (decrease in the sum of squares of residuals) will be large. On the other hand, if the blast models are similar, then there will only be a small increase in likelihood. This is formalized by considering the ratio of the likelihoods for the four- and two-parameter cases (Silvey 1970).

Twice the difference in the log-likelihoods, sometimes called the deviance, turns out to be the difference in the residual sums of squares of

models. Under the null hypothesis that the two-parameter case is the correct one, this quantity (the deviance) will be distributed as a chi square variable with 4 – 2 = 2 degrees of freedom:

$$\text{Log-likelihood} = 2(LL_{(H0)} - LL_{(H1)})$$

By multiplying the difference between the likelihoods by a factor of 2, the quantity will be distributed as the familiar chi square statistic. This can then be assessed for statistical significance by using standard chi square significance levels. The degrees of freedom for the test will equal the difference in the number of parameters being estimated under the alternative and null models. For most blasting cases, two parameters will be estimated under the null model, and four under the alternative model, and therefore the chi square will have two degrees of freedom.

The assessment of the significance using a chi square statistic ultimately places the burden of final assessment on the investigator. Depending on the nature of the investigation and the required confirmation, the actual level to be regarded as the critical significance level will be seen to vary. However, in statistical investigations of this kind, it is common to observe the 90% threshold (chi square percentage chance of difference) as being the point beyond which a 'difference' can be confidently reported.

As the manual computation of a likelihood ratio test is a very long-winded process, the results of this investigation are the product of a bespoke variant of the University of Leeds developed *Blast Log* program that has been specifically designed to analyse and compare surface and underground blast vibration data.

5 WHITWELL QUARRY RESULTS

Figure 1 displays the conventional (square root) scaled-distance model for all the blast vibration data collected from Whitwell quarry. As can be seen, both a poor standard error and correlation coefficient are visible (the derived values are 0.92 and 0.58 respectively). In contrast, Figure 2 displays all the collected data, subdivided according to either surface or underground recordings. Immediately apparent, but coming as no surprise, is the fact that the two data subsets present themselves as unique models in their own right. Visual inspection supports the presence of two data sub-sets, but what is not clear is the degree to which the datasets can be labelled different.

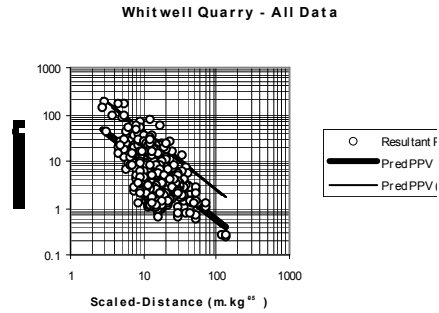

Figure 1. Whitwell quarry scaled-distance regression model – all data.

The results of subjecting the data to a likelihood ratio test can be seen in the lower right of Figure 2. The test derives a log-likelihood ratio of 7.94, which, when compared with the chi squared distribution, indicates a percentage chance of difference of approximately 98%. In other words, there is an approximate 98% chance that the surface and the underground recording data will be different from each other. This will come as no real surprise as the existence of a difference is easily appreciated way before the application of the likelihood ratio test, but what the test has provided is a credible statistic as to that degree of difference.

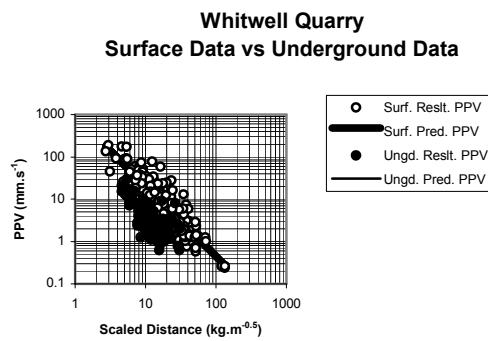

Figure 2. Whitwell quarry surface data versus underground data with likelihood ratio test output.

Regarding Figure 2, a clearer relationship between the surface and the underground data can be achieved by removing from the surface dataset all those data recorded that do not lie on the same immediate transmission path to the location of the boreholes. This is realistically achieved by filter-

ing the surface data so as to include only those data recorded at the surface adjacent to the collars of the boreholes, and then make statistical comparisons in turn with the data recorded from the triaxial arrays located at both the bottom and at the mid-depth of the boreholes. Not only will this limit the amount of data scatter associated with the surface recordings, it will give a clearer indication of how the results vary with depth.

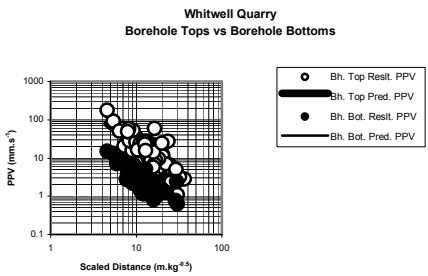

Figure 3. Whitwell quarry borehole surface data versus borehole bottom data with likelihood ratio test output.

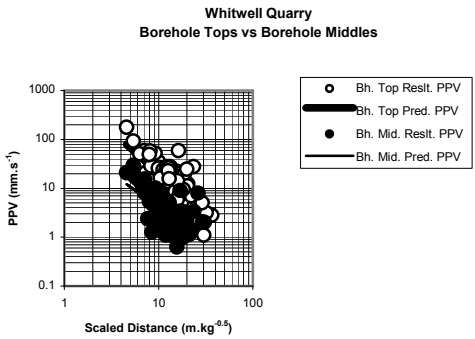

Figure 4. Whitwell quarry borehole surface data versus borehole middle data with likelihood ratio test output.

Figure 3 displays the data recorded at the top of the boreholes juxtaposed with the data recorded at the bottom. Figure 4 displays the same surface data juxtaposed with the data from the middle of the boreholes. Figure 5 compares the data from the middle of the boreholes with the data from the bottom. In addition, each figure also displays the results of the likelihood ratio test, and a summary of all the individual scaled-distance model summary statistics is reported in Table 1.

Looking at Figures 3 and 4, a clearer indication of the relationship between the surface readings and the underground readings is established. Of most interest is the fact that the apparent differences are solely in the intercept values for the regression lines, with the gradients remaining approximately parallel and constant. This is reiterated by the site factor B values reported in Table 1. Here, it can be seen that the fluctuations in the surface and underground values are minimal, with such variations most likely being the product of random data scatter, especially as it can also be seen from Table 1 that the returned standard error and correlation coefficient values (apart from 'all data') remain reasonably constant across the board.

In both Figures 3 and 4, the results of the likelihood ratio tests provide statistical verification of the disparity between the datasets, with the chi square percentage chance of differences running at approximately 99% for the surface and borehole bottom data (Fig. 3) and at approximately 97% for the surface and borehole middle data (Figure 4). As such values far exceed the 90% threshold required confidently to report a 'difference', such visually apparent differences are supported with true statistical confidence. By contrast, the comparison between the borehole middle recordings and the borehole bottom recordings (Figure 5) returns a percentage chance of difference of approximately only 40%, which actually implies a 60% chance of data communality. Visual inspection of Figure 5 suggests that this minor variation is most likely the effect of data scatter rather than any underlying mechanism.

Therefore, having established and statistically proven the relationship between the surface and the underground scaled-distance models, it now becomes possible to exploit this relationship and use the surface data to predict the vibration levels at depth.

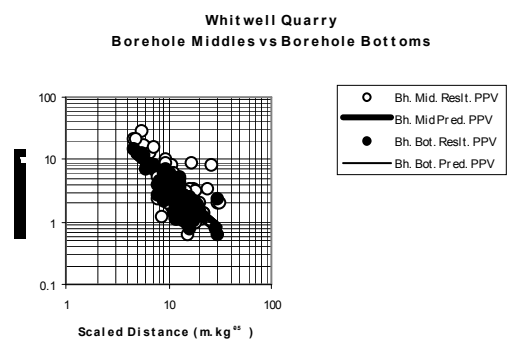

Figure 5. Whitwell quarry borehole middle data versus borehole bottom data with likelihood ratio test output.

Table 1. Whitwell quarry all scaled-distance models – summary statistics.

	All data	All data	All data	Borehole data	Borehole data	Borehole data
		Surface	Underground	Top	Middle	Bottom
Data count	547	355	192	133	110	82
Standard error	0.92	0.52	0.51	0.52	0.55	0.41
Correlation coeff.	0.58	0.88	0.70	0.75	0.67	0.79
Site factor A	170.35	952.64	102.97	973.69	104.26	110.94
Site factor B	–1.25	–1.67	–1.44	–1.65	–1.40	–1.53

Table 2. Maximum instantaneous charge weights that are compliant for *X*% of blasts to be less than 12 mm/s from both surface and underground derived scaled-distance models.

	Maximum Instantaneous Charge Weights (kg) compliant with X% of all blasts to be less than 12mm/s: (SURFACE)			X% of all blasts to be less than 12mm/s: (UNDERGROUND)		
Distance (m)	**95%**	**98%**	**99.9%**	**95%**	**98%**	**99.9%**
100	17.11	13.21	6.81	225.36	180.94	103.12
125	26.73	20.64	10.64	352.13	228.72	161.13
150	38.50	29.72	15.32	507.07	407.11	232.02
175	52.40	40.46	20.86	690.17	554.13	315.81
200	68.44	52.84	27.24	901.45	723.76	412.49
250	106.94	82.56	42.57	1408.52	1130.87	644.51
300	153.99	118.89	61.29	2028.26	1628.46	928.09

Table 3. Example peak particle velocity predictions for a distance of 200 m with a maximum instantaneous charge weight of 60 kg.

Example PPV predictions for a distance of 200m with a M>I>C> of 60kg.				
	% chance			
Predicted PPV	50	95	98	99.9
Surface (mm/s)	4.18	9.78	12.00	20.83
Underground (mm/s)	0.95	2.20	2.72	4.65

6 CHARGE WEIGHT IMPLICATIONS

The identification of a clear and distinct relationship between the vibration readings taken on the surface to those taken underground has important repercussions for the derivation of limit compliance charge weights. Table 2 presents the MIC compliant weights that observe upper confidence levels of 95, 98 and 99.9% not to exceed vibration levels of 12 mm/s with respect to the scaled-distance regression models for both the top of the

boreholes ('surface') and the bottom of the boreholes ('underground'). As can be seen, the disproportion of the values is very clear and highlights the extreme overconservatism that would occur in conventionally using surface vibration recordings and models to derive charge weights that are compliant with limitations placed upon underground structures. As an example, if it were decided that the interpretations of not exceeding the 12 mm/s maximum PPV level would be the 98% probability line (i.e. a 1 in 50 chance), then, at distances closer than 250 m (based on surface monitoring), the maximum instantaneous charges would have to be reduced either by double decking or by splitting benches. However, what is clear from this study is that from underground monitoring at a distance of 100 m there exists a less than 1 in 1000 chance of exceeding the 12 mm/s maximum PPV level.

The magnitude of the difference in PPVs measured on the surface with those measured underground becomes even more apparent if we consider the vibration likely to arise as a result of the same charge weight at a similar distance (see Table 3). Here, we see that, if again we define compliance as 12 mm/s PPV at the 98% probability limit, then there is an even chance of a surface reading in excess of 4.18 mm/s. However, for an underground reading, the even chance becomes 0.95 mm/s and indeed the equivalent 1 in 1000 chance is only 4.65 mm/s.

7 SUMMARY AND CONCLUSIONS

The work at Whitwell quarry in Derbyshire as outlined in this paper has been successfully built upon the original work carried out at Taffs Well quarry in South Wales. Having already established that a PPV limit of 12 mm/s to prevent damage was too restrictive, this work has clearly demonstrated in a statistically rigorous way that, when blast vibrations formed by quarry blasts and monitored at a surface location are compared with those monitored at a underground location, they form two distinct groups. It is therefore statistically incorrect to combine the two sets of data and treat them as one for predictive purposes. Furthermore, it has been shown that, if only surface monitoring is carried out in order to limit blasting vibrations at an underground location, this may well give rise to a completely unwarranted level of protection for the structure concerned and inevitably lead to the unnecessary sterilisation of reserves.

REFERENCES

Andrieux, P., McKenzie, C., Heilig, J. & Drolet, A. 1996. The impact of blasting on excavation design – a geomechanics approach. In *Proc. annual conference on explosives and blasting techniques.*

Birch, W., Pegden, M., West, R. & White, T. 2004. The application of likelihood ratio test to blast vibration analysis. *Proc. 30th annual conference on explosives and blasting technique, New Orleans, LA, 2004*: Vol 2. Cleveland, Ohio: International Society of Explosives Engineers.

Clover, A.W. 1986. Appraisal of potential effects of surface blasting on a rock tunnel, with particular reference to the Tai Lam Chung water tunnel, Hong Kong. *Rock engineering and excavation in an urban environment. Proc. of conference held in Hong Kong, IMM*. Hong Kong: Freeman Fox & Partners (Far East).

Dowding, C.H. 1977. Lifeline viability of rock tunnels: empirical correlations and further research needs. In *Proc. Technical Council on Lifeline Earthquake Engineering, speciality conference on current state of knowledge of lifeline earthquake engineering, Los Angeles*: 320–337.

Farnfield, R.A. & White, T.J. 1993. Research into the effects of surface mine blasting on buildings: long term monitoring projects. *The Mining Engineer inc. Trans. Inst. Mining Eng.* 152(380): 319–323.

Fisher, R.A. 1925. Theory of statistical estimation. *Proc. Cambridge Philosophical Society* 22: 700–725.

Kaslik, M., Birch, W.J. & Cobb, A. 2000. The effects of quarry blasting on the structural integrity of a disused railway tunnel. In *Proc. 27th annual conf. on explosives and blasting techniques, Orlando, February 2000*: Vol 2, 199–211.

Labreche, D.A. 1983. Damage mechanisms in tunnels subjected to explosive loads. *Seismic design of embankments and caverns. Proc. of symposium sponsored by ASCE Geotechnical Engineering Division in conjunction with ASCE National Convention, Philadelphia, Pennsylvania*: 128–141.

Langefors, U & Kihlstrom, B. *The Modern Technique of Rock Blasting*: 288.

New, B.M. 1989. Trial and construction induced blasting vibration at the Penmaenbach road tunnel. Transport and Road Research Laboratory. Department of Transport. Research report 181.

Nichollis, H.R., Johnson, C.F. & Duvall, W.I. Blasting vibrations and their effects on structures. *Mines Bull.* 656: 1871.

Olson, J.J., Fogelson, D.E., Dick, R.A. & Hendrickson, A.D. 1972. Ground vibrations from tunnel blasting in granite. Bureau of Mines report of investigations 7653, US Department of the Interior.

Sakurai, S & Kitamura, Y. 1977. Vibration of tunnel due to adjacent blasting operation. In *Int. symp. on field measurements in rock mechanics, Zurich*.

Silvey, S.D. 1970. *Statistical Inference*. London: Chapman and Hall.

Smith, M.C.F. 1986. Construction and blasting methods at Kornhill site formation works. *Rock engineering and excavation in an urban environment. Proc. of conference held in Hong Kong, IMM*.

Tunstall, A.M. 1997. Damage to underground excavations from open pit blasting. *Trans. Inst. Min. Metall. (Sect A: Min. Industry)* 106: A19–A24.

Brighton Conference Proceedings 2005, R. Holmberg et al

Evaluation of blast-induced vibrations - a case study of the Istanbul Cendere region

C. Kuzu & T. Hudaverdi
Istanbul Technical University, Mining Engineering Department, Turkey

ABSTRACT: Mine-induced effects from quarries create considerable problems in the vicinity. In particular, blast-induced ground vibrations are a challenging issue that gives rise to strong public reaction. For very rapidly growing cities, like Istanbul, the required raw materials for the construction industry are supplied from quarries in the vicinity or from inside the city. With further growth in the population density, many quarries that are now rural will be in suburban areas, and this development will make the situation more difficult. There is still no national standard regarding vibration evaluation, especially in complex problems such as blast-induced vibrations. In this paper, blasting operations and their possible environmental effects are defined. Methods for blast prediction and commonly accepted criteria for preventing damage are introduced. Monitored vibration data collected in three neighbouring quarries are evaluated, and the well-known procedures of the US Department of Interior Office of Surface Mining Reclamation and Enforcement (OSMRE) are discussed and demonstrated with examples.

1 INTRODUCTION

In recent years, blast-induced vibrations have emerged as an important environmental effect for mining operations. This environmental effect creates more problems, especially in aggregate mining. Usually, aggregate mines (quarries) are operated near the cities in order to reduce transportation costs. In developing cities like Istanbul, quarries outside the city are gradually approaching residential areas because of rapid city growth. Naturally, blast-induced vibrations cause significant problems between quarries and the residents near the quarries.

Generally, the main factors affecting blast-induced vibrations are the distance to the blasting area and the explosive charge per delay. Controlled blasting techniques should be applied if blasting activities are carried out near residential areas. If the distance between the blasting area and buildings is small, generally the precautions are focused on limiting the explosive charge. The relation between blasting factors and blast-induced vibrations should be considered in order to determine additional precautions. Table 1 presents the factors that affect vibration levels.

Table 1. Controllable and uncontrollable factors affecting the vibration levels (Atlas Powder Company 1987).

		Degree of importance		
		V	I	L
Controllable factors				
1	Charge weight per delay	X		
2	Length of delay	X		
3	Detonator accuracy	X		
4	Burden and spacing		X	
5	Stemming type and length			X
6	Charge length and diameter			X
7	Inclination of holes			X
8	Direction of initiation		X	
9	Charge weight per blast			X
10	Charge dept			X
11	Usage of denonating cord		X	
12	Initation system		X	
Uncontrollable factors				
1	Topography		X	
2	Specifications of overburden		X	
3	Atmospheric conditions			X
V = very important; I = important; L = less important.				

As can be seen in Table 1, the most important parameters for controlled blasting are the limitation of the explosive charge per delay and the parameters serving to produce new free faces in the braking process.

Almost all new investigation procedures use the peak particle velocity (PPV) as the main element for examining the vibrations. In addition, peak values of particle acceleration (PPA) and displacement (PPD) should be investigated.

2 PROCEDURES OF OSMRE

Over the years, a number of criteria relating ground motion to structural damage have been established and implemented with varying degrees of success. One of them, based on peak particle velocity, has been developed as a regulation by the US Department of Interior Office of Surface Mining Reclamation and Enforcement (OSMRE) (Rosenthal & Marlock 1987). These are presented in the following chapters and also discussed by means of a case study. In all procedures, as mentioned above, peak particle velocity plays an important role. These procedures are:

- Limiting particle velocity.
- Scaled distance equation.
- Modified scaled distance.
- Blasting level chart.

2.1 Limiting particle velocity criterion

In this way (30CFR Section 816.67(d)(2)(i)), the vibration values of each shot are recorded (OSMRE, Federal Regulations). Each of the three components of the particle velocity is analysed according to limit values shown in Table 2. If three components of the particle velocity are under the limit value, the blast is defined as harmless for the environment. In this way, there is no need for frequency knowledge.

Table 2. Maximum permitted particle velocities at various distances from the blast site.

Distance (ft)	Maximum peak particle velocity (in/s)
0–300	1.25
301–5000	1.00
≥5001	0.75

2.2 Scaled distance equation criterion

In this way (30CFR Section 816.67(d)(3)(i)), the maximum charge amount W (kg) is determined per delay time by the scaled distance factor (SD). This factor is determined in relation to the distance between shot and measurement stations, D (m), to fix the maximum charge amount (OSMRE, Federal Regulations). Table 3 presents the maximum amount of explosives that can be shot per 8 ms or greater delay as a function of distance and scaled distance factor. The equation used to determine scaled distance (SD) is presented below:

$$SD = DW^{-0.5} \quad (1)$$

where D = slope distance between the shot and the nearest dwelling; SD = scaled distance factor; and W = total weight of explosives per minimum of 8 ms delay.

Scaled distance values are general values and very conservative. Sometimes, this approach can limit explosive usage too much, and this method does not require that blasts be monitored.

Table 3. Maximum amount of explosive/delay as a function of distance from blast and scaled distance factor (Hustrilid 1999).

Distance (ft // m)	Scaled distance limit value $SD = D/W^{0.5}$ ($ft/lb^{0.5}$)	Maximum charge for 8 ms delay (lb // kg)
100 // 30.48	SD = 50	4.0 // 1.8140
150 // 45.72	0–300 ft	9.0 // 4.0815
200 // 60.96	(0–90 m)	16.0 // 7.2576
250 // 76.20		25.0//11.3375
300 // 91.44		36.0//16.3260
400 // 121.92	SD = 55	53 // 24.0355
600 // 182.88	301-5000 ft	119 //53.9665
800 // 243.84	(91-1500 m)	212 //96.1420
1000 // 304.80		331//150.1085
2000 // 609.60		1322//599.5270
4000//1219.20		5290//2399.015
5500//1676.40	SD = 65	7160//3247,612
6000//1828.80	>5001 ft	8521//3864.273
10,000//3048.0	(>1501m)	23,700//10747.95

2.3 Modified scaled distance criterion

As explained in the second procedure, the 'scaled distance equation criterion' is most restrictive and the only non-site-specific criterion. The 'modified

scaled distance criterion' and subsequent 'blast level chart criterion' are more effective under more critical conditions (30CFR Section 816.67(d)(3) (i)&(ii)). In this procedure, a statistical approach avoids the need for regular monitoring of every shot and allows the blaster to produce a site-specific scaled distance factor (OSMRE, Federal Regulations). By doing so, this new site-specific scaled distance factor gives the blaster a chance to predict peak particle velocity, v, by the so-called attenuation formula:

$$v = H(\mathrm{SD})^{-\beta} \tag{2}$$

where v = peak particle velocity; SD = scaled distance factor; and H and b = site factors.

It should be noted that, for a valid statistical analysis, 30 or more data pairs (v–SD) are required. Once a modified scaled distance has been established, it must be renewed from time to time in relation to the advance of quarry faces.

2.4 Blasting level chart criterion

In the fourth procedure (30CFR Section 816.67(d)(4)(i)), the blasting level chart presented in Figure 1 is used to determine the maximum allowable ground vibration if the predominant frequency is known (OSMRE, Federal Regulations). As can be seen, for frequencies greater than 30 Hz the maximum allowable particle velocity reaches 2 in/s. This is related to the fact that the natural frequencies of structures are in the low-frequency range (4–12 Hz). This procedure is least restrictive, permits highest velocities, maximum explosive charges and shortest distances and provides greatest freedom in blast design. However, every shot with peak particle velocity and frequency values must be monitored.

3 EVALUATION OF DATA THROUGH THE THIRD AND FOURTH PROCEDURES

Akdaglar quarry located in the Cendere Valley in Istanbul (quarry B in Fig. 2) was chosen for investigation of blast-induced vibrations. The valley is situated within Kemerburgaz and Ayazaga, with a length of 10 km and a width of 0.5–3 km. The main material of these quarries is micaeous sandstone with a specific gravity of 2.7–2.8 g/cm^3, a Mohs hardness of 6–7 and a compressive strength of 1300–1500 kg/cm^2. This investigation was realised according to the third procedure (modified scaled distance criterion) and the fourth procedure (blasting level chart criterion).

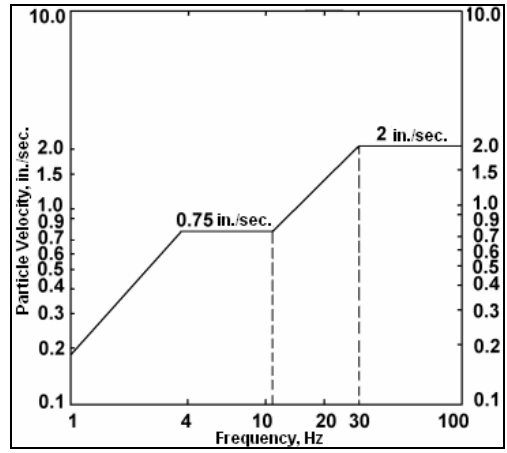

Figure 1. Peak particle velocity versus frequency limits.

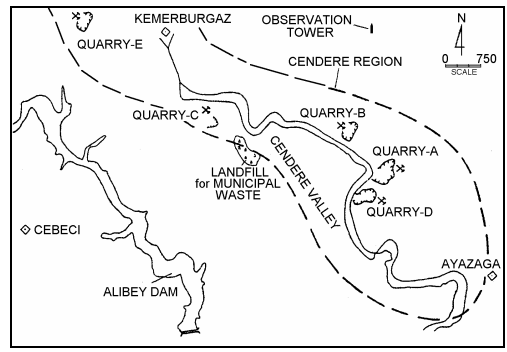

Figure 2. Location of quarries in the Cendere region (Kaynarkan *et al.* 1999).

The records belonging to 33 different production shots are presented in Table 4, and a statistical equation based on the dataset is developed (Kuzu 2001):

$$\mathrm{PPV} = 113.61\mathrm{SD}^{-1.1546} \tag{3}$$

The equation, directly related to the location of the quarry and the specifications of the shots, should be modified according to the development of the production area of the quarry. That is, geographic and geological variations must be factors in modifying the scaled distance equation (White & Farnfield 1993).

Based on this statistical approach, it is observed that the scaled distance varies between 1.47 and 12.07 m/kg$^{0.5}$, and the lower part of this range shows high peak particle velocities. As shown in Table 4 and Figure 3, the maximum PPV value is 68.5 mm/s for SD = 2.61 m/kg$^{0.5}$ at a 50 m distance from the site of the shot (shot 27).

A similar shot (shot 24, D = 50 m, W = 350 kg, SD = 2.67 m/kg^{05}, PPV = 61.1 mm/s) gives a similar result. These lower values, which are gained by modification of scaled distances through statistical analysis, make it possible to work with more explosives. For safer results, the aim is to set a second control with the fourth procedure (blasting level chart), especially for the lower SD values, which brings frequency considerations into the investigation too.

For that reason, two records (shots 15 and 17) are chosen and evaluated according to the fourth procedure (Fig. 4A, B):

– shot 15 (D = 35 m, W = 216 kg, SD = 2.38 m/kg^{05}, maximum PPV = 49.5 mm/s) is recognised as safe;
– Shot 17(D = 21 m, W = 145 kg, SD = 1.74 m/kg^{05}, maximum PPV = 41.7 mm/s) is recognised as not safe owing to one of its PPV component frequency values at 16 Hz.

Table 4. Seismic records of the observed blasts.

Data of prediction formulae											
Shot no.	D (m)	W (kg)	SD (m/kg^{05} // ft/lb^{05})	PPV (mm/s // in/s)	f_T–f_V–f_L (Hz)	Shot no.	D (m)	W (kg)	SD (m/kg^{05} // ft/lb^{05})	PPV (mm/s // in/s)	f_T–f_V–f_L (Hz)
1	65	209	4.49 // 9.93	17.3 // 0.6811	19–34–14	**18**	25	287.5	1.47 // 3.25	40.1 // 1.5787	23–37–15
2	80	262	4.94 // 10.92	24.7 // 0.9724	>100–22–15	**19**	32	425	1.55 // 3.42	46.5 // 1.8307	23–37–15
3	175	450	8.24 // 18.22	16.9 // 0.6654	28–37–20	**20**	100	350	5.34 // 11.81	13.5 // 0.5315	18–20–26
4	70	318	3.92 // 8.67	37.7 // 1.4843	21–22–17	**21**	150	300	8.66 // 19.13	8.11 // 0.3193	22–32–18
5	100	370	5.19 // 11.48	10.9 // 0.4291	28–16–18	**22**	35	400	1.75 // 3.86	51.1 // 2.0118	30–35–22
6	100	315	5.63 // 12.44	14.8 // 0.5827	15–16–14	**23**	75	325	4.16 // 9.19	36.1 // 1.4213	18–25–22
7	195	309.5	11.08 // 24.49	4.08 // 0.1606	21–20–22	**24**	50	350	2.67 // 5.90	61.1 // 2.4055	30–23–25
8	80	233.1	5.23 // 11.57	13.8 // 0.5433	64–24–11	**25**	180	300	10.35 // 22.96	5.1 // 0.2008	23–26–27
9	55	364.5	2.88 // 6.365	65.5 // 2.5787	23–28–26	**26**	90	250	5.69 // 12.57	15.1 // 0.5945	20–24–18
10	100	311	5.67 // 12.52	10.2 // 0.4016	22–20–23	**27**	50	365.5	2.61 // 5.77	68.5 // 2.6969	16–39–37
11	80	337	4.35 // 9.62	20.8 // 0.8189	9.7–14–13	**28**	210	350	11.22 // 24.80	12.3 // 0.4843	20–19–13
12	115	267	7.03 // 15.55	7.54 // 0.2969	27–17–17	**29**	120	161	9.45 // 20.89	12.5 // 0.4921	30–17–32
13	155	320	8.66 // 19.14	8.58 // 0.3378	17–15–20	**30**	225	347	12.07 // 26.68	7.92 // 0.3118	11–20–16
14	50	215	3.40 // 7.53	31.7 // 1.248	28–27–14	**31**	220	370	11.43 // 25.27	4.13 // 0.1626	15–N/A–23
15	*35*	*216*	*2.38 // 5.26*	*49.5 // 1.9488*	*64–43–21*	**32**	45	291	2.63 // 5.82	35.1 // 1.3819	27–22–17
16	30	329.5	1.65 // 3.65	51.8 // 2.0394	18–24–16	**33**	34	163	2.66 // 5.88	46.5 // 1.8307	47–39–26
17	*21*	*145*	*1.74 // 3.85*	*41.7 // 1.6417*	*34–47–16*						

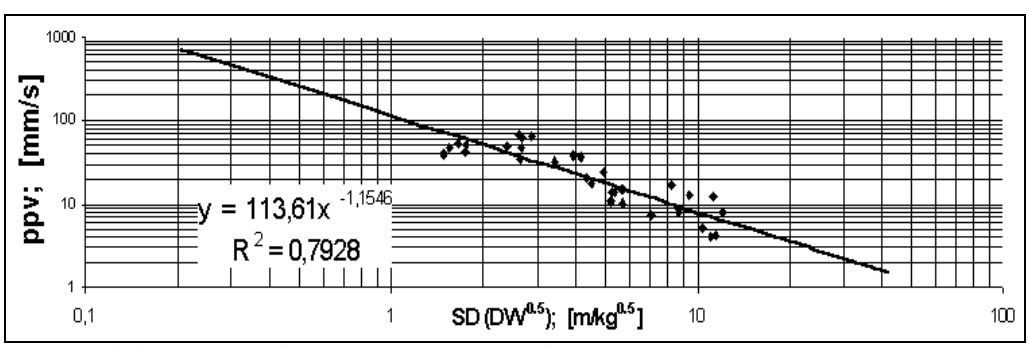

Figure 3. Calculated correlation between SD and particle velocity (x = SD).

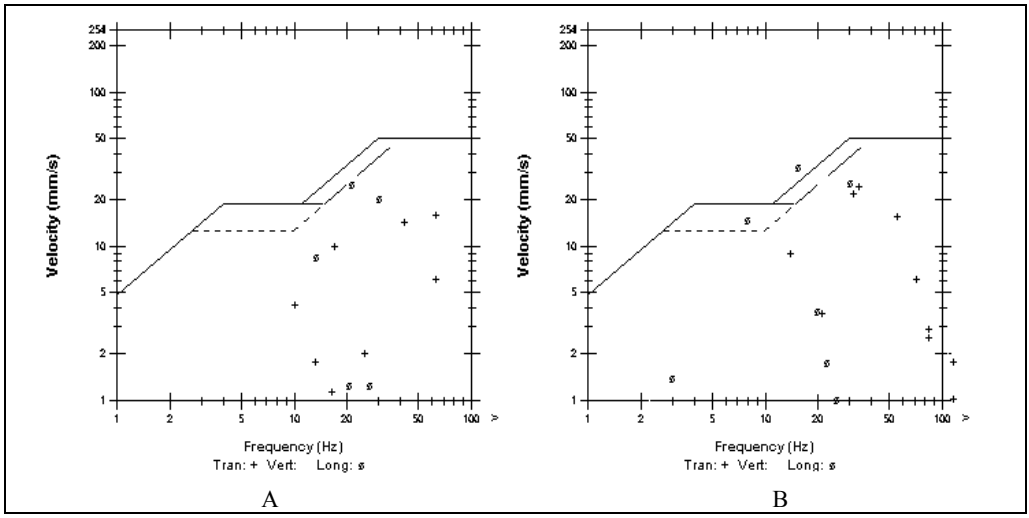

Figure 4. Evaluation of the records by using the blasting level chart criterion.

1 CONCLUSIONS

In particular, a risk analysis must be made in order to determine the factors that can affect the blasting operations and the vibration level. There are still methods based on experimental data to enable this. A significant method, among others, is to produce a PPV predictor dependent on site-specific seismic indicators which are obtained by monitoring shots in the field to find out the optimal conditions for blasting.

Therefore, some quarries are already making use of the concept of scaled distance and establishing quarry-specific vibration predictors such as the case presented in this paper. Comprehensive procedures in this regard have been developed by OSMRE, and one of the OSMRE procedures, the fourth procedure, gives the blasters a great opportunity to use maximum loadings at shortest distances where highest peak particle velocities are allowable. On the other hand, the third procedure enables the blasters to calibrate the blasting work and also makes it possible to predict peak particle velocities in relation to factors *D* and *W*. That is, the third procedure eliminates the conservative restrictions of the first and second procedures and gives more flexibility. Therefore, these two procedures should be used to complement each other.

REFERENCES

Atlas Powder Company 1987. Explosives and Rock Blasting.

Hustrulid, W. 1999. Blasting Principles for Open Pit Mining: Vol. 1: Balkema.

Kaynarkan et al. 1999. Investigation in Cendere (Kemerburgaz–Ayazaga–Istanbul) aggregate–concrete–asphalt production basin. In 2nd national symp. on aggregate mining, Istanbul, January 1999.

Kuzu, C. 2001. The investigation of the blast-induced vibrations occuring in different formations in aggregate mines around Istanbul and the examination of the effects of the vibrations on near residential areas. ITU research project. Istanbul.

OSMRE, Code of Federal Regulations, 30 CFR Part 700. http://www.osmre.gov/regindex.htm; and/or http://www.access.gpo.gov/nara/cfr/cfr.

Rosenthal, M.F. & Marlock, G.L. 1987. Blasting Guidance Manual: OSMRE.

White, T.J. & Farnfield, R.A. 1993. Computers and blasting. Int. Trans. Inst. Mining and Metallurgy. Section A, January–April, A19–A24.

Session 5

Brighton Conference Proceedings 2005, R. Holmberg et al

Structure response to trench and road blasting

V.L. Rosenhaim
Mineral and Explosives Engineering, New Mexico Institute of Mining and Technology, Socorro, NM, USA

C.H. Dowding
Civil and Environmental Engineering, Northwestern University, Evanston, IL, USA

C.T. Aimone-Martin
Mineral and Civil Engineering, New Mexico Institute of Mining and Technology, Socorro, NM, USA

ABSTRACT: Crack and structure response to construction trench blasting was measured in a wood-frame house with a stucco exterior. Blasts at distances between 232 and 368 m produced peak particle velocities (PPV) and airblast overpressures (AB) of 9 mm/s and 0.02 kPa (123 dB) respectively. Structure response velocities were measured at an upper corner and two mid-walls, as were changes in the width of a crack at a window corner in the east mid-wall. Structure responses were correlated with PPV and AB, which arrived simultaneously, complicating the distinction between the two. Crack responses were correlated with long-term changes in temperature and humidity as well as PPV and AB. Wall strains from out-of-plane bending and in-plane shear were computed from upper corner structure response and compared with failure strains for dry wall. As has been found in other studies, calculated strains were far lower than those required to crack dry wall, and the environmentally induced crack response from temperature and humidity was far greater than that caused by blast-induced ground motion or airblast overpressures.

1 INSTRUMENTATION TO MEASURE STRUCTURE RESPONSE

Figures 1 and 2 show the instrumentation locations within, and exterior to, the structure. The location of the interior, single-component velocity transducers placed in the upper (S2) corner, lower (S1) corner, and at the mid-wall in the living room east and north walls are indicated in Figure 1. LARCOR™ multicomponent seismographs were used digitally to record four channels of seismic data. The exterior (master) unit consisted of a triaxial geophone and an airblast microphone. The geophone, buried to 150 mm depth, was oriented so that the radial, R, and transverse, T, components were respectively perpendicular to and parallel with the east wall containing the instrumented crack. This orientation is based upon recording motions that are parallel with one of the translation axes of the house rather than the traditional direction relative to the vibration source. The airblast microphone was installed 250 mm above the ground surface and was used to record the pressure pulses transmitted through the air.

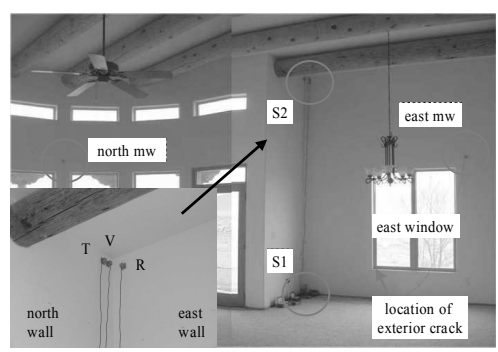

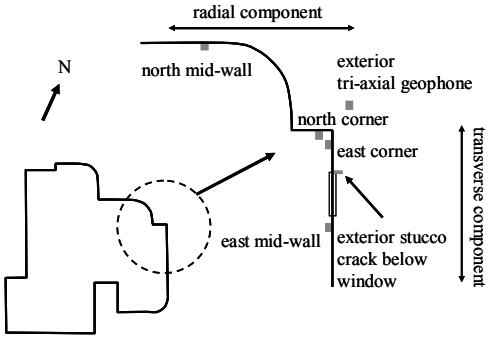

Figure 1. Plan view of the instrumented house (top) and the locations of the velocity transducers to measure the structure response (bottom).

Figure 2. Locations of the crack and null sensors at the corner of the east window.

Both the S1 and S2 seismographs were connected to clusters of three single-axis transducers in the upper and lower interior corners and adjoining wall at mid-wall (north or east wall), as shown in Figure 1. These transducers were affixed to the walls using hot glue to minimise damage during removal. The three corner transducers, labelled R, T and V in Figure 1 (bottom right), measured whole-structure motions in the horizontal radial (nominal east-west), transverse (nominal north-south) and vertical directions respectively. The mid-wall transducers measured horizontal motions during wall flexure or bending. Further details of this system can be found in work by Aimone-Martin *et al.* 2002).

To measure the effect of blasting and climate conditions (temperature and humidity) on changes in the width of an existing exterior crack, Kaman™ eddy-current gauges were installed as shown in Figure 2, and data were collected using a field computer. Each Kaman gauge consisted of mounting brackets, an active element and a target plate. Gauges were mounted in brackets affixed to the stucco exterior across an existing crack (crack gauge) and on an uncracked surface (null gage). The crack gauge was installed with each mounting bracket placed on either side of the crack. Operation of eddy-current gauges has been described elsewhere (Dowding and Siebert 2001, Dowding and Snider 2003, Hitz and Welsby 1997).

The three seismographs and the field computer were connected in series, with the exterior seismograph acting as the master (triggering) unit and all other systems as slave units. The Kaman gauge system was programmed to sample crack displacement every hour in response to environmental changes. Upon triggering, the master seismograph delivered a 1 V pulse via the serial cable to activate and begin recording dynamic data during blasting events. This produced seismograph and dynamic crack/null gauge records that were time correlated to the nearest 0.001 s, which is critical for analysis of structure and crack response.

2 GROUND MOTION AND AIRBLAST ENVIRONMENT

Blasting, ground motion and airblast data are given in Table 1. Figure 3 shows blast locations as shot layouts for trench and road blasts. Maximum charge weights per 8 ms delay varied between 1.4 and 88 kg, and scaled distances (SD) from 31.2 to 253.8 m/kg$^{1/2}$. Peak particle velocities (PPVs) in the horizontal direction, recorded in the ground outside the structure, ranged from 1 to 9 mm/s. The frequencies of the maximum excitation pulse varied between 3 and 18 Hz. The PPVs are well below the generally accepted threshold for cosmetic hairline cracks of 12–19 mm/s for excitation frequencies below 10 Hz. Airblast overpressures ranged from 0.002 to 0.02 kPa.

3 DYNAMIC CRACK AND STRUCTURAL RESPONSE

Nine time histories of excitation and response for

blasts on 12/30a and 1/28 are shown in Figures 4 and 5. The upper three time histories are displacements of the crack and relative displacements between the upper and lower transducers in the radial and transverse directions. The next three below them are the velocity time histories of the response of the upper wall corners in the radial and transverse directions, and the mid-wall response (in the radial direction). The bottom three time histories are the excitation by airblast and radial and transverse ground motion. Transverse is parallel with the east wall containing the crack.

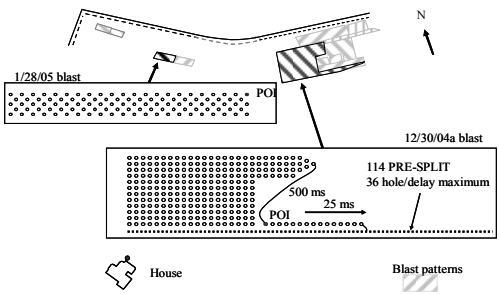

Figure 3. Typical trench shot pattern showing location relative to the structure and point of initiation (POI).

These two events produced the highest ground motions (12/30a) and the highest airblast overpressure (1/28). In neither case were the ground motion and airblast peaks separated for a sufficient time to draw unequivocal conclusions. On 12/30 the peak airblast and ground motion occurred at the beginning of the time history, and on 1/28 the peak airblast occurred near the end of the event while there was still significant ground motion. These two events involved the highest airblast overpressures of 0.02 kPa (120 dB or 0.003 lbf/in^2) and 0.014 kPa (117 dB or 0.002 lbf/in^2), which are relatively small compared with the allowable 0.07 kPa (133 dB or 0.01 lbf/in^2).

The natural frequency of the structure can be estimated from the last several seconds (after second 6) of the radial structural motions excited by the 1/28 blast. These responses occur without significant ground motion or airblast excitation. S2 in the radial and the east mid-wall velocity responses are similar and indicate a natural frequency of some 8 Hz. Motions in the transverse direction are not as consistent but do contain significant motion in the same frequency range. During seconds 2–4, fairly uniform excitation occurs at a frequency of 6 Hz in both the radial and transverse directions. It is during this time that the maximum mid-wall and S2 radial response is observed.

Peak responses (y axes) are plotted in Figure 6 versus various excitation possibilities (x axes). All points are the response peak (y) that follows the maximum excitation peak (x) by less than one response period. This comparison differs from finding the maximum peak response in the record first and then the preceding peak excitation within the preceding response period. The distinction is important as it allows observation of the significant drivers of response.

In Figure 6, the first row of graphs compares S2, the velocity responses in the radial (perpendicular to the east wall containing the crack) and transverse (parallel with the east wall) directions, with the time-correlated maximum PPVs in the

Table 1. Summary of blast details and measured ground and airblast.

Shot Date	Distance From Structure	Charge Weight/Delay	Scaled Distance	Peak Particle Velocity	Frequency at the PPV	Airblast	Number of holes	Shot Type
	(m)	(kg)	(m/kg$^{1/2}$)	(mm/sec)	(Hz)	(kPa)		
9/16/2004	296	2.27	196.5	0.889	8.5	0.002	78	trench
9/17/2004	296	1.36	253.8	1.016	14.6	0.008	86	trench
9/21/2004	368	11.34	109.3	3.175	3.7	0.006	320	road cut
9/23/2004	299	3.40	162.2	1.143	14.2	0.002	360	trench
09/30/04	290	8.39	100.1	3.048	7.7	0.0012	290	road cut
12/30/04a	293	87.98	31.2	9.270	5.2	0.014	311/109 PS	road cut/PS
12/30/04b	293	18.14	68.8	3.175	4.5	0.006	48	road cut
1/27/05a	232	14.52	60.9	3.937	18.2	0.004	154	trench
1/27/05b	232	14.52	60.9	1.397	9.8	nd	42	trench
1/28/2005	257	22.68	54.0	3.683	10.2	0.02	103	trench

PS – presplit shot detonated with road cut.

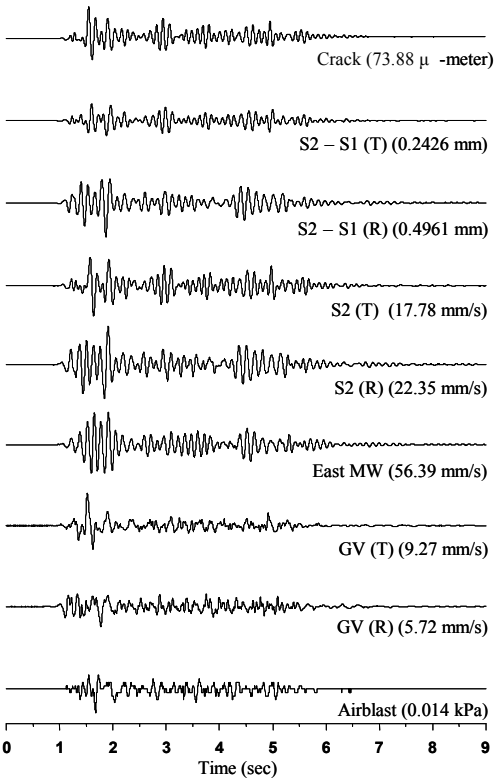

Figure 4. Time histories of structural response (upper five), excitation of ground velocities and air pressure and crack motions for event on 12/30/04a.

same directions. In the second row, dynamic crack responses are compared with the maximum PPVs perpendicular to and parallel with the wall containing the crack (radial and transverse directions respectively).

In the third row, dynamic crack responses are compared with maximum differential wall displacements between top (S2) and bottom (S1) transducers. Finally, at the bottom, peak crack responses are compared with the maximum airblast overpressures, which are omnidirectional.

For this structure and range of excitation frequencies, the PPV in the direction parallel with the wall containing the crack (east wall) appears to be the best predictor of crack response. Row 2 comparison in Figure 6 shows that the peak crack response is not predicted at all by the maximum radial ground motions (PPV direction perpendicular to the wall containing the crack). It is the transverse motions parallel with in-plane shearing that open and close the crack. The next closest predictor would be the differential displacement in the direction parallel with the east wall, shown in the third row. However, it is only a slightly better predictor than the differential displacement in the perpendicular direction. Finally, the airblast peak is the least able to predict the maximum crack response. The relatively small effect of the peak airblast overpressure may result from the small pressures generated at this test house by these events.

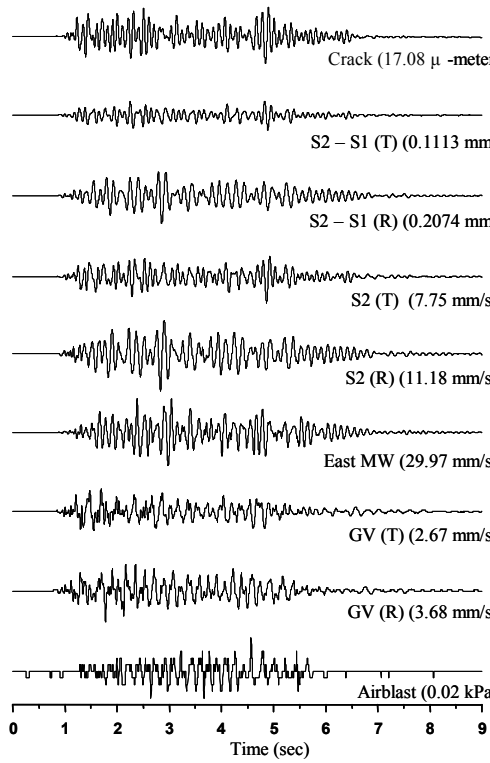

Figure 5. Time histories of structural responses (upper five), excitation of ground velocities and air pressure and crack motions for event on 1/28/05.

3 STRAINS

The magnitude of induced strains in structure components determines the likelihood of cosmetic cracking in residences. Global strains may be estimated from differential displacements at the upper, S2, and lower, S1, corners, in directions parallel with and perpendicular to the plane of the wall of interest, the east wall in this case. Velocity time histories at S1 and S2 are first integrated to obtain displacement time histories, then the largest time-correlated difference between corner

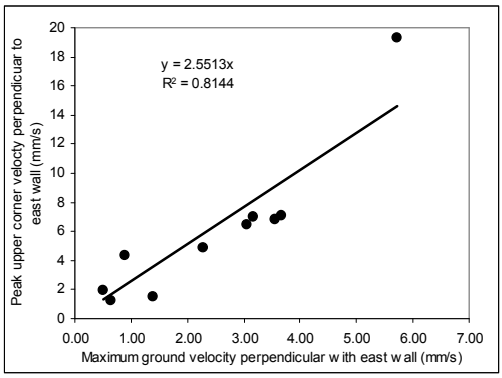

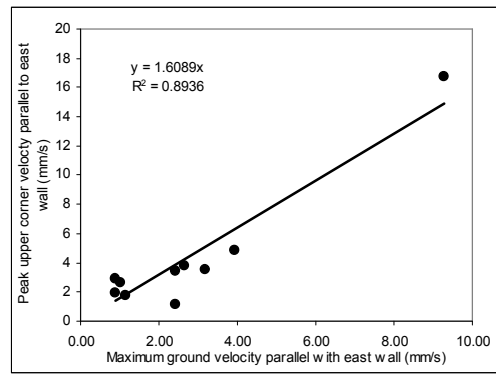

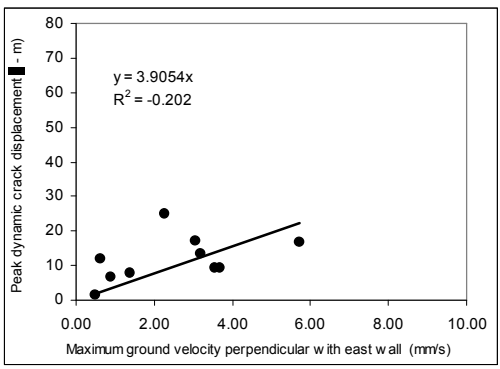

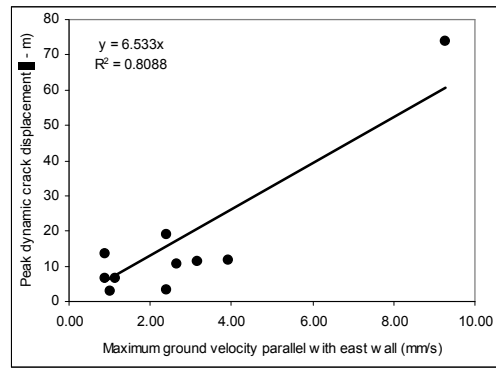

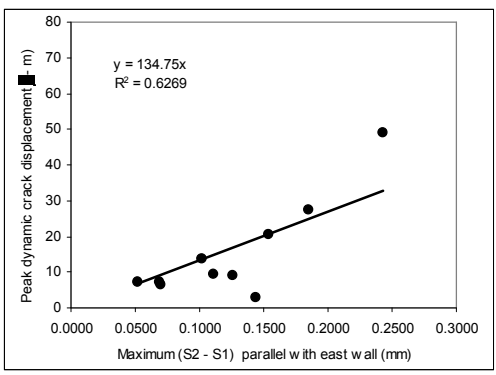

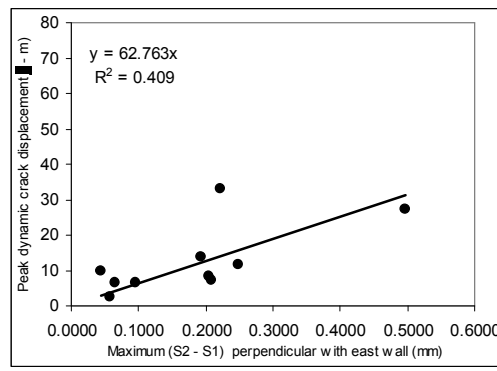

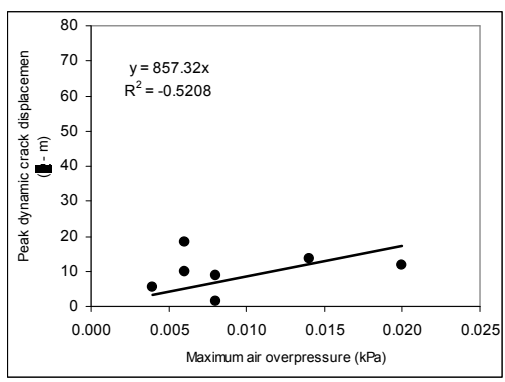

Figure 6. Structural and crack responses to peak ground motions, relative displacements and airblast.

responses (S2 – S1) is employed to calculate strain. Examples of such differential displacement time histories are presented as the second and third time histories from the top in Figures 4 and 5.

First consider differential displacements in the direction parallel with the east wall, which produce 'in-plane' shear and related tensile strains. Global shear strain is determined by the following:

$$\gamma_{\max} = \left(\frac{\delta_{\max}}{L} \right) \quad (1)$$

where γ_{max} = global shear strain (microstrains or 10^{-6}); δ_{max} = maximum differential displacement parallel to the wall, S2 – S1 (in or mm); and L = height of the wall subjected to strain (in or mm).

In-plane tensile strain, $\varepsilon_{L\ max}$, is calculated from the global shear strain by the equation

$$\varepsilon_{L\ \max} = \gamma_{\max} (\sin\theta)(\cos\theta) \quad (2)$$

where θ is the interior angle of the longest diagonal of the wall subjected to strain with reference to the horizontal. Angle θ is calculated by taking the inverse tangent of the ratio of wall height to wall length.

Next, consider differential displacements in the direction perpendicular to the east wall, which produce 'out-of-plane' bending strains and the related extreme fibre tensile strains. While the lower wall, S1, is well coupled to the ground, or 'fixed', the upper wall, S2, and the roof can have varying degrees of 'fixity', ranging from relatively unconstrained to highly fixed. Bending strain is most conservatively estimated with the fixed–fixed analogy because this mode shape predicts the highest strains in walls per unit of maximum relative displacement (Dowding 1996). These out-of-plane bending strains can be calculated as

$$\varepsilon = \left(\frac{d 6 \delta_{\max}}{L^2} \right) \quad (3)$$

where ε = bending strain in the walls (microstrains or 10^{-6}), and d = distance from the neutral axis to the wall surface, or half the thickness of the wall subjected to strain (in or mm).

Table 2 summarizes the maximum calculated strains induced by ground motion excitation. The maximum recorded whole-structure differential displacement was 0.4961 mm in the plane of the east wall containing the crack. The maximum calculated in-plane global shear strains and related tensile strains were 135 and 67 microstrains. The maximum calculated out-of-plane bending strain was 38 microstrains. The range of failure in the gypsum core of dry wall is 300–500 microstrains (Dowding 1996). Using the maximum observed tensile strain of 67, the factors of safety against cracking were 4–7 for the interior dry wall. Therefore, any cracks in interior dry wall cannot be attributed to blasting strains.

Table 2. Calculated wall strains compared with maximum ground velocities and crack motions.

Shot Date	Maximum differential wall displacement, S2-S1 (mm)		Maximum shear strain (micro-strain)	Maximum in-plane tensile strain (micro-strain)	Maximum bending strain (micro-strain)	Maximum ground velocity (mm/s)		Peak Crack Motion
	perpendicular to east wall	parallel to east wall	east wall	east wall	east wall	Radial	Transverse	(micro-m)
9/16/2004	0.04369	0.06937	11.94	5.94	3.99	0.635	0.889	18.67
9/17/2004	0.05733	0.14406	15.67	7.79	4.63	0.508	1.016	6.33
9/21/2004	0.19285	0.10249	28.02	26.22	12.52	3.175	2.413	19.72
9/23/2004a	0.09627	0.05179	26.32	13.09	6.74	0.889	1.143	14.13
09/30/04	0.24890	0.12602	68.05	33.84	18.00	3.048	2.413	20.69
12/30/2004a	0.49607	0.24261	135.63	67.44	38.44	5.715	9.271	73.89
12/30/2004b	0.20403	0.15352	55.78	27.74	14.78	2.286	3.175	25.07
1/27/2005a	0.22157	0.18476	60.56	30.12	16.07	3.556	3.937	34.65
1/27/2005b	0.06573	0.06974	17.97	8.94	4.40	1.397	0.889	10.69
1/28/2005	0.20744	0.11113	56.7	28.2	18.25	3.683	2.667	17.09

4 .LONG-TERM OR ENVIRONMENTAL AND WEATHER-INDUCED CRACK RESPONSE

Long-term changes in crack width are presented in Figure 7, along with outside temperature and humidity for a period of 135 days (3240 h). In general, long-term crack movement followed the trend in exterior humidity, while short-term (or 24 h) movement was consistent with diurnal temperature. When the humidity increased, the crack opened (positive change), whereas a sudden increase in temperature produced crack closure.

Weather front effects such as rain (shown with the vertical dashed line in Figure 7) had the largest influence on long-term crack movements. By contrast, daily crack movements were strongly affected by the early morning sun on the eastern wall exposure. The large variation in crack width over a half-day cycle can be seen in the graphical expansion of hours 2233–2760. The largest measured change over this daily cycle was some 300 μm.

Peak-to-peak dynamic crack motions (red bar) from the most significant blast on 12/30/04a are compared with daily and long-term environmental effects in the bottom two graphs in Figure 7.

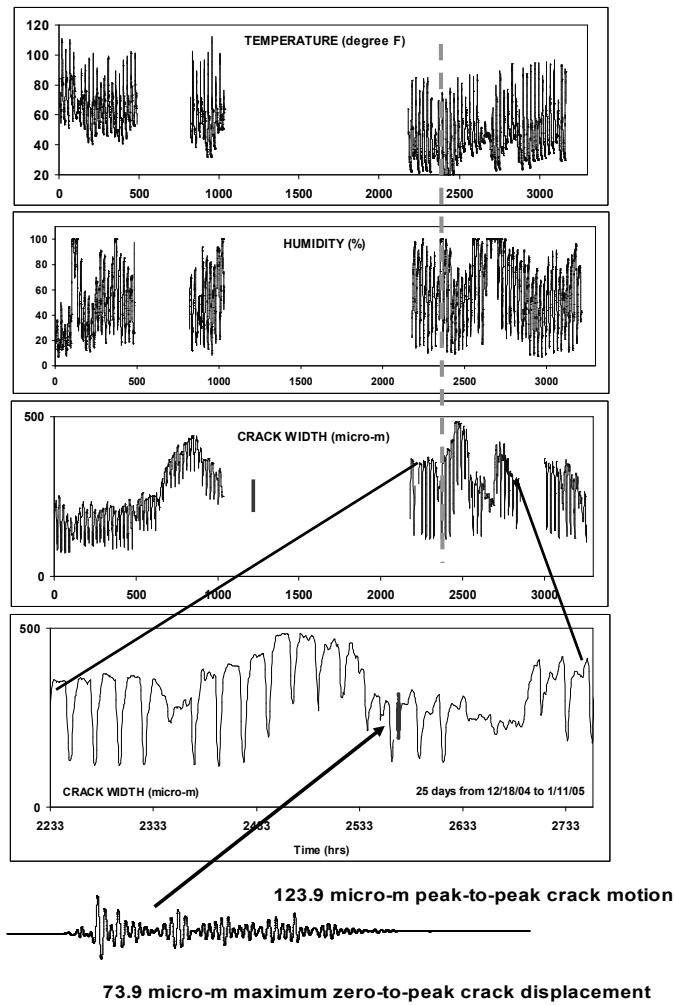

Figure 7. Comparison of long-term crack response with outside temperature and humidity, showing relative dynamic crack motions during the blast on 12/30/04a.

The daily change of 300 µm (peak to peak) exceeded the largest change in crack width during blasting (74 µm zero to peak and 124 peak to peak) on 12/30/04a. Furthermore, the greatest overall change in crack width for the duration of the study was 410 µm, as shown on the 133 day portion of Figure 7. This weather-induced change in crack width is the largest contributing factor to crack extension and widening over time. The effect of blasting vibration on changes in crack widths is negligible compared with the influence of climate. Hence, blasting is unlikely to be the source of stucco cracking.

It is important to measure crack response for several months to observe the long-term environmental effects. As shown in Figure 7, in spite of significant diurnal solar heating on the east wall, the longer-term or seasonal effects were still larger (300 and 410 µm respectively).

5 CONCLUSIONS

Peak airblast levels did not occur at the same time as peak crack and structure response, and were thus poor predictors of crack. This lack of influence may result from the low level of airblast generated in this study at the test structure. Similar studies at higher airblast overpressure levels are needed.

On the other hand, peak ground motion levels did occur slightly ahead of the peak crack and structure response, and were better predictors of crack response than were airblast overpressures.

The natural frequency of the structure was determined from free vibration response as 8 Hz, which is within the expected range of 4–12 Hz.

The calculated maximum in-plane tensile wall strain from ground motion excitations was 67 microstrains. The calculated maximum mid-wall bending strain was 38 microstrains. The maximum airblast-induced mid-wall bending strains could not be distinguished. These blast-induced strains are far less than the 300–500 microstrains necessary for dry wall failure.

The crack response to environmental changes was far greater than the response to dynamic excitation from either ground motions or airblast overpressures. The maximum recorded crack width response from blasting was 74 and 123 µm zero to peak and peak to peak respectively. During the 133 day study, the daily temperature and humidity induced crack peak-to-peak responses of up to 300 µm, and the seasonal environmental effects induced crack responses of 410 µm.

6 ACKNOWLEDGEMENTS

This project was sponsored and supported by Salls Brothers Construction, Inc. The authors acknowledge the guidance and contributions of John White of Salls and students participating on this project from Northwestern University and New Mexico Institute of Mining and Technology. Crack monitoring equipment was supplied by the Infrastructure Technology Institute at Northwestern University, which was supported by a block grant from the US DOT to commercialise innovative instrumentation. More information on autonomous crack monitoring instrumentation is available on the internet from www.iti.northwestern.edu/acm

REFERENCES

Aimone-Martin, C.T., Martell, M.A., McKenna, L.M., Siskind, D.E. & Dowding, C.H. 2002. Comparative study of structure response to coal mine blasting. Report prepared for US Office of Surface Mining Reclamation and Enforcement, Pittsburgh, PA. Available at www.osmre.gov/blastingindex.htm

Dowding, C.H. 1996. *Construction Vibrations*: 620 pp. Originally published by Prentice Hall, NJ, reprints now available at Amazon.com

Dowding, C.H. & Siebert, D. 2001. Control of construction vibrations with an autonomous crack comparometer. *Proc. conference on explosives and blasting technique*, *European Federation of Explosives Engineers, Munich, Germany*: Balkema. Reprints of article available at www.iti.northwestern.edu/acm

Dowding, C.H. & Sinder, M. 2003 New approach to control of vibrations generated by construction in rock and soil. In *Proc. soil and rock America symposium, 12th Pan American conference on soil mechanics and geotecnical engineering and 39th US rock mechanics symposium, Massachusetts Institute of Technology (MIT)*: Essen, Germany, VGE. Reprints of article available at www.iti.northwestern.edu/acm

Hitz, T. & Welsby, S.D. 1997. True position measurement with eddy-current technology. *Sensors Magazine*: 13.

Brighton Conference Proceedings 2005, R. Holmberg et al

Safe seismic zone determination during construction pit excavation for a university library in Split, Croatia

D. Vrkljan, Z. Ester & M. Dobrilović
Faculty of Mining, Geology and Petroleum Engineering, University of Zagreb, Croatia

ABSTRACT: Construction of the University library was performed within the University campus of Split (Croatia) on a densely populated location. Excavation of a construction pit for the library was carried out by blasting to a maximum depth of 17m. The nearest building, the Faculty of Electrical and Mechanical Engineering and Shipbuilding, was only 18m away from the construction site. For determination of a safe seismic magnitude of blasting, trial blasting was performed. The allowed quantity of explosive charge per interval of ignition was estimated by an original method, respecting the world-known norms (ISO 4866, DIN 4150, US BM 8507, and BS 7385) which determine permitted ground velocity oscillations depending on frequency. Based on the results of seismic monitoring on the location of the trial blasting, safe blasting magnitudes and other safety measures for the execution of excavation works were developed.

1 INTRODUCTION

The University Library Project within the University campus of Visoka-Split is being carried out in an area with a large number of buildings of more than 10 floors. The surface area of the construction pit is 5,370 m^2 (68 x 79 m). Due to the hard rock ground, formation excavation has been made by blasting. The depth of the excavated area ranges from 18m on the northern edge to 8m on the southern edge. Test blasting was performed to

Figure 1. Construction pit.

determine seismic values safe for the surrounding buildings (housing, university and public buildings). Based on the results of seismic monitoring, safe drilling and blasting parameters were set.

2 GEOLOGICAL AND GEOTECHNICAL CHARACTERISTICS OF ROCK IN THE CONTRUCTION PIT

According to the Primary Geological Map—Location Split, and the geo-engineering survey of the surrounding terrain and excavation pits, the terrain of the location consists of gravelled material (AF) beneath which follow alluvial clays of quaternary age (Q_{el}), whereas in the basis are deposits of eocene flysch ($E_{2,3}$). The depth of the gravelled material is 50-140 cm. The depth of alluvial clay is 70 cm, north side, and 120cm, south side. The basic rock of flysch consists of clayey marls with interlayers of flysch. The layers are fragmented, dipping toward Northeast under angle between 50° and 85°. Geological strength index (GSI) of flysch deposits ranges from 40 to 60 points.

3 TEST BLAST FIELD

The test blast field is in the south-east corner of the construction pit. Emulsion explosive, reinforced with aluminium dust in 50mm cartridge (elmulexal), was used in blasting drills of 64 mm in diameter. Specific consumption of explosives in the test field was 0.40 kg/m^3. Seismic data were collected in 6 directions (Figure 2).

Ground oscillation velocities were measured on portable seismographs: White digital Seismograph Mini-Seis II 2D2G; INSTANTEL BlastMate II DS-447; INSTANTELL Blast-Mate III"; and INSTANTEL MiniMate.

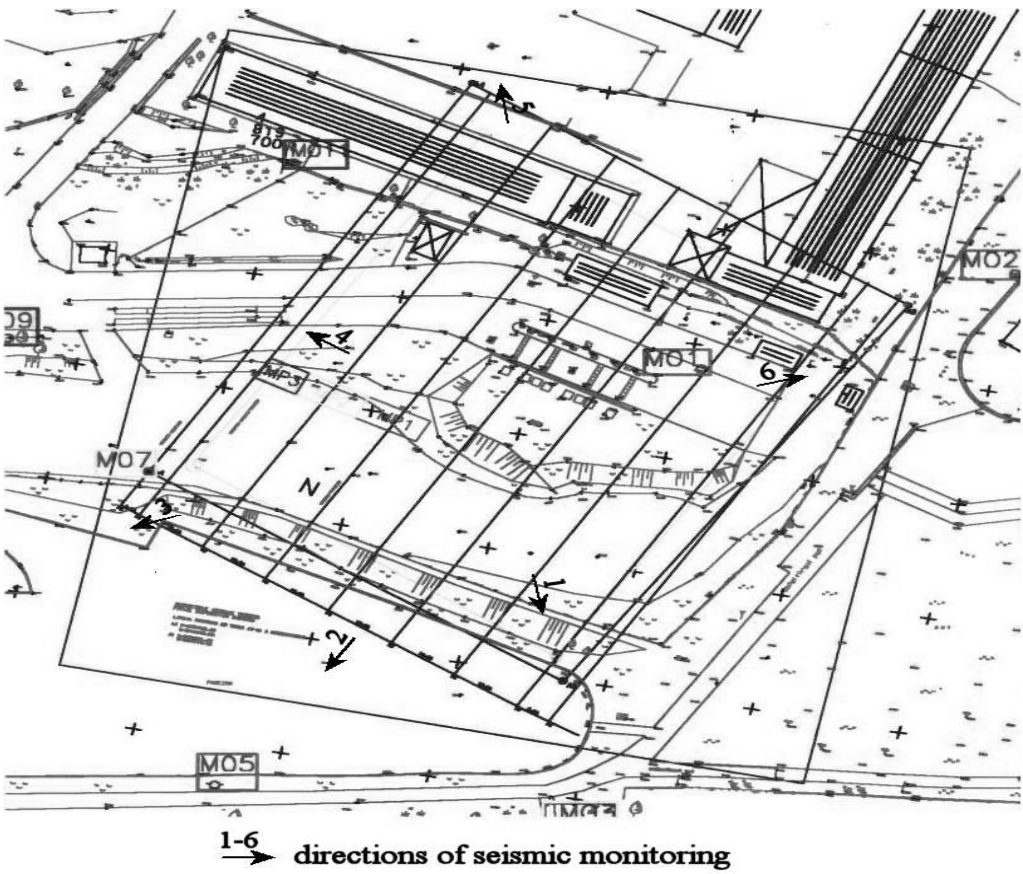

Figure 2. Situation map of construction pit with location of test blast field (MP) and measurement points (MO).

3.1 Calculation of allowed explosive charge quantities

Calculations were conducted for two critical directions:

- Northeast direction toward the Faculty of Electrical and Mechanical Engineering and Shipbuilding.
- Southeast direction toward a non-detached housing facility.

The relationship between ground oscillation velocities, the quantity of explosive charges and the distance of the observation point from the blast field is shown in this formula by M.A. Sadovsky:

$$v = k(\frac{\sqrt[3]{Q}}{R})^n \ \text{(cm/s)} \qquad (1)$$

where v=ground oscillation velocity (cm/s); k =the coefficient of the type of blasting; Q=the maximum quantity of explosive charges for each delay (interval) of firing (kg); R =the distance of the observation point from the blast field (m) and n=the coefficient of restrainment of the seismic waves.

At every blasting job, the variables R and Q are known, and from measurement results, the resultant ground oscillation velocities at the observation points are calculated. Coefficients k and n are precisely calculated using a system of equations, which can be found when the ground oscillation velocities are measured at two observation points during one blasting. Taking into consideration the state of the endangered objects, the adjusted ground oscillation velocity permitted was v_d=1.5 cm/s.

3.2 Safe seismic blasting zones

Based on the calculation of allowed explosive charge quantities per degree of firing in two critical directions, safe seismic zones were determined inside the construction pit (Figure 3). Other directions and buildings placed on this direction are relatively distanced and therefore non-critical for blasting regime determination. A corresponding blasting regime was determined for each zone.

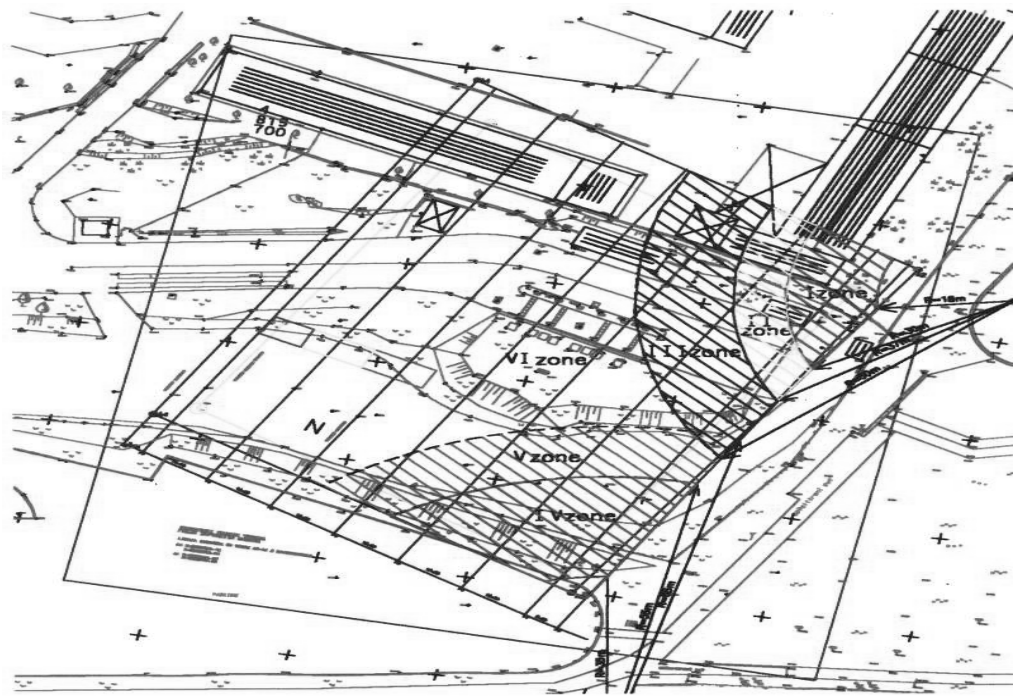

Figure 3. Situation map of construction pit with safe seismic zones (I-VI).

Table 1. Drilling and blasting values in seismic zones.

Zone	Degrees of firing	Explosive charge per degree, kg	Explosive total quantity, kg	Excavation depth, m	Drilling geometry		Volume break per blasthole, m^3	Explosive charge kg/m^3
					Burden m	Spacing, M		
1st	2	0.5	1.0	3.5	1.0	1.2	4.2	0.24
2nd	1	2.4	2.4	3.5	1.3	1.5	6.8	0.35
3rd	2	4.8	9.6	8.0	1.7	2.0	27.2	0.35
4th	2	1.2	2.4	5.0	1.5	1.5	11.2	0.22
5th	1	7.2	7.2	5.5	1.7	2.2	20.6	0.35
6th	1	12.0	12.0	7.5	1.9	2.4	34.2	0.35

First to third safe zones were determined, containing the Faculty of Electrical and Mechanical Engineering and Shipbuilding at the Northeast corner of the construction pit.

The Fourth and fifth zone were determined, containing a housing facility to the south-east of the construction pit.

4 DRILLING AND BLASTING VALUES

Drilling and blasting values are based on the results of seismic measurements during test blasts, efficiency results of testing blasts taking into consideration the surrounding (populated) area of blasting.

The primary goal was to perform drilling-blasting activities without endangering people and property in the vicinity of the construction pit. Another goal was obtaining adequate technical and economical values of blasting, like fragmentation of discharged material (ISEE (1998), Sandvik Tamrock Corp (1999)), discharging of material and optimising of blasting effects (which was in this case slightly neglected for the sake of environmental protection).

The blasting drill was set at 64 mm, which was optimum under conditions of seismic limitations.

The geometry of drilling was variable upon seismic zones (Ester&Vrkljan, 2004). The majority of drilling and blasting operations was conducted in the sixth seismic zone. For the sixth seismic zone, burden w=1.9m was set with a drill spacing of a=2.3m. In other seismic zones, the geometry of drilling was decreased accordingly to optimise favourable effects of blasting. Table 1 shows drilling and blasting values for each safe seismic zone (I-VI).

During the blasting process, constant control seismic observation was conducted on the endangered buildings. Generally speaking, the frequency of component seismic waves was of a very favorable range over 50 Hz. Undesirable frequencies below 10 Hz were not recorded.

The recorded ground oscillation velocities were within the range prescribed by the norm DIN4150.

'Elmulexal' emulsion explosive reinforced with aluminium dust was used in cartridges of 50 mm in diameter. Median specific consumption of drilling = 3.1 m^3/m and median explosives charge of 0.34 kg/m^3 was achieved.

5 CONCLUSION

The excavation of the construction pit for the University Library in Split was conducted in a densely populated urban area, without causing damage to surrounding objects through seismic effects of blasting, by following proper procedure:

- test blast with seismic measurements,
- construction pit definition in safe seismic zones with corresponding blasting regime set upon seismic measurement results of test blasts,
- firing of explosive charges in multiple millisecond intervals / degrees of firing,
- limitations to maximum allowed explosive charge quantity per blast field,
- continuous seismic monitoring of critical surrounding objects,
- reduction of explosive charge quantity per degree of firing in case of excessive ground oscillation velocities on surrounding objects, ensuring ground oscillation velocities inside allowed range.

REFERENCES

Ester, Z., Vrkljan, D. 2004 Technology of Excavation by Blasting Construction Pit for University Library

in Split, Faculty of Mining, Geology and Petroleum Engineering, University of Zagreb, Zagreb, October.
ISEE. 1998. Blasters Handbook. 479 -508. Cleveland, Ohio.
Sandvik Tamrock Corp, 1999, Rock Excavation Handbook for Civil Engineering, 188-204.